NOVEL LONG NON-CODING RNA MIR205HG: AN ESOPHAGEAL TUMOR-SUPPRESSIVE HEDGEHOG INHIBITOR

by

Jee Hoon Song

A dissertation submitted to Johns Hopkins University in conformity with the requirements for the degree of Doctor of Philosophy

Baltimore, Maryland

March, 2015

© 2015 Jee Hoon Song

All Rights Reserved

ABSTRACT

Esophageal adenocarcinoma (EAC) is one of the most rapidly increasing cancers in Western countries, but its underlying molecular mechanisms have not yet been fully elucidated. Recently, the discovery of long non-coding RNAs (lncRNAs) has added a new layer of complexity to the molecular architecture, identifying these molecules as emerging key regulators of diverse biological pathways. Increasing evidence shows that lncRNA dysregulation can lead to many diseases, including cancer, but their potential involvement in EAC is not yet well-understood.

In this study, we used massively parallel RNA sequencing to identify a set of lncRNAs that were differentially expressed in esophageal cancers *vs.* normal esophageal epithelia. After a rigorous filtering procedure, miR205HG was found to be strikingly downregulated in EAC cell lines and tissues. *In vitro* assays in EAC cell lines demonstrated that overexpression of miR205HG inhibited cell proliferation, cell cycle progression, and colony formation. Moreover, *in vivo* mouse xenograft experiments using miR205HG-stably transfected EAC cells revealed that forced miR205HG overexpression inhibited tumor growth in nude mice. We then posited that miR205HG's mechanism of action involved the Hedgehog (HH) signaling pathway, since miR205HG and SHH expression levels were found to inversely correlate in patient EAC (r= -0.73) and BE (r= -0.83) tissues. Furthermore, miR205HG overexpression was shown to inhibit sonic hedgehog (SHH) transcription and translation. In summary, our findings suggested that

miR205HG is involved in the development and/or progression of EAC and offers potential as a therapeutic target and a prognostic biomarker.

Readers:

Stephen J. Meltzer, M.D.

William H. Matsui, M.D.

Thesis Advisor:

Stephen J. Meltzer, M.D.

ACKNOWLEDGEMENTS

This project has been the joy and the bane of my existence for the last four years. I could not have persistently pursued this project without abundant support and encouragement from my mentors, colleagues, friends, and family.

First and foremost, I would like to thank my thesis advisor and mentor, Dr. Stephen J. Meltzer, for his support, guidance, and endless patience throughout this process. My time as a graduate student was certainly memorable: there were moments of pure accomplishment and happiness, but a simple PCR result could also push me into a bottomless abyss. I would like to sincerely thank Dr. Meltzer for helping me through those difficult times. When I was sad, he would hand me tissues to dry my tears (and lend me his shoulder to cry on); when I was frustrated, he would listen to my venting (and lend me his shoulder to punch on); and when I was hungry, he would slip me a bagel or two (and lend me his lunch to munch on). His everlasting trust in me and his guidance have made this whole journey worthwhile. He always encouraged me to try new ideas and has allowed me to develop independence. I will always be grateful for all the opportunities he has provided me, for he has shaped me into the person I am today.

I also want to thank the members of our laboratory, especially Dr. Yulan Cheng, Dr. John Abraham, and Binbin Huang. It has been an honor to have their support, friendship and care. I could not have asked for better supporters and friends. Next, I would like to thank the members of my thesis committee, Drs. William H. Matsui, Michael Goggins, and

John Abraham (again!) for their expertise and insightful suggestions. It has been a privilege to have their advice and guidance, which have formed an essential contribution to my project. In addition, I would like to thank Colleen Graham and Leslie Lichter of the Cellular and Molecular Medicine program at the Johns Hopkins University School of Medicine for their kind support.

Last, but certainly not least, I would like to thank my parents for their unconditional love and endless hours of supporting me. They are my everything, and I am blessed to have them. I could never have survived those endless winters in Baltimore without their daily phone calls, or their continuous supply of nourishing Korean food. Because of them, although we may have been living far apart geographically, I never felt alone in Baltimore.

TABLE OF CONTENTS

LIST OF FIGURES

LIST OF TABLES

LIST OF ABBREVIATIONS

3'UTR: 3' untranslated region

BE: Barrett's esophagus

BMP4: Bone morphogenetic protein 4

EAC: Esophageal adenocarcinoma

EC: Esophageal cancer

ESCC: Esophageal squamous cell carcinoma

GAPDH: Glyceraldehyde 3-phosphate dehydrogenase

GERD: Gastroesophageal reflux disease

HH: Hedgehog

LncRNA: Long non-coding RNA

miRNA: MicroRNA

NcRNA: Non-coding RNA

NE: Normal esophagus

qRT-PCR: Quantitative real-time polymerase chain reaction

RNA-seq: RNA sequencing

SHH: Sonic hedgehog

SOX9: SRY (sex determining region Y)-box 9

INTRODUCTION

Esophageal cancer (EC) is the 6th-leading cause of cancer death worldwide, with almost 15,000 deaths per year in the U.S. and 5-year survival rates of only 15% (van Soest *et al.*). EC is classified into two major histopathologic subtypes: esophageal squamous cell carcinoma (ESCC) and esophageal adenocarcinoma (EAC). ESCC and EAC represent two separate entities, with distinct etiologies and pathologies that entail somewhat different detection and therapeutic strategies. ESCC is the most frequent EC subtype internationally and predominates in eastern Asia and eastern and southern Africa, whereas EAC predominates in Western populations (Enzinger *et al.*). Nicotine and alcohol abuse are the major risk factors for ESCC, and though its incidence has decreased over the past 20 years, the overall prognosis of patients with ESCC remains poor (Enzinger *et al.*).

We focus on EAC in this study because it is the leading EC subtype in the United States. EAC generally develops in patients with chronic gastroesophageal reflux disease (GERD) and its premalignant lesion, Barrett's esophagus (BE) (Schneider *et al.*). Arising secondary to chronic GERD-induced inflammation, BE is characterized by the replacement of the normal squamous esophageal lining by a specialized metaplastic columnar epithelium. The precise prevalence of BE has been difficult to determine, since most BE patients are asymptomatic; however, BE is estimated to affect somewhere between 1.6 and 6.8 percent of the general population (Gilbert *et al.*). A diagnosis of BE confers an 11- to 30-fold increase in EAC risk, although only a minority of BE patients

ever develop EAC (Gilbert *et al.*). Typically, chronic GERD patients are screened for BE which, if found, necessitates subsequent periodic endoscopic (EGD) surveillance. EACs detected at surveillance EGD are diagnosed at earlier stages and exhibit better survival than those found outside of surveillance (Corley *et al.*). Unfortunately, not all patients presenting with EAC have previously been under surveillance or diagnosed as having BE (Sharma *et al.*). Thus, most EACs are detected at advanced stages, leading to very poor survival rates. Clearly, a better understanding of the molecular basis of BE and EAC is needed for earlier detection, effective individualized cancer risk evaluation, and improved outcome. The study of long non-coding RNAs (lncRNAs) in cancer progression as missing puzzle pieces now appears essential to our understanding of the molecular genetic scaffolding of all cancers in general, and of EAC progression in particular. By studying lncRNAs, we thus expect to gain comprehensive new insights into the molecular basis of BE and EAC, along with potential novel strategies toward their early detection and treatment.

CHAPTER ONE: IDENTIFYING A NOVEL LONG NON-CODING RNA DYSREGULATED IN BARRETT'S ESOPHAGUS AND ESOPHAGEAL ADENOCARCINOMA

INTRODUCTION

The central dogma of molecular biology dictates that the flow of genetic information transfers from DNA to RNA to protein. However, the emergence of long non-coding RNAs (lncRNAs), which do not get translated into proteins, alters this dogma by rendering RNA as the final recipient of genetic information. Although lncRNAs were once considered merely wasteful transcriptional byproducts, the recent advent of high-throughput genomic sequencing technologies has revealed an extensive network of lncRNAs transcribed in human genome. These lncRNAs, whose functions are largely undefined, have immense potential to elucidate unknown facets of the molecular architecture.

LncRNAs belong to the larger family of non-coding RNAs (ncRNAs), which are divided into two classes: structural ncRNAs and regulatory ncRNAs. Structural ncRNAs include tRNAs, rRNAs, and small nucleolar RNAs (snoRNAs); regulatory ncRNAs include microRNAs (miRNAs), PIWI-interacting RNAs (piRNAs), and lncRNAs (Nie *et al.*). Regulatory RNAs are subclassified based on their length, wherein miRNAs are the shortest (22-23 nts) and lncRNAs are the longest (>200 nts). According to the

GENCODE v19 catalog of human lncRNAs, there are approximately 13,800 lncRNA genes that produce 24,000 lncRNA transcripts (Walsh *et al.*). However, because approximately 97% of the genome is transcribed, this universe is likely to be much larger, with some estimates placing the total number of lncRNAs at several hundred thousand (Nie *et al.*). As with protein-coding RNAs, lncRNA transcription is performed by RNA polymerase II, although some lncRNAs are transcribed by RNA polymerase III. Again similar to mRNAs, many lncRNAs are spliced, polyadenylated, and 5'-capped; but unlike mRNAs, most lncRNAs localize to the nucleus (Nie *et al.*).

Recent studies have demonstrated that lncRNAs maintain key cellular processes, including protein-coding gene regulation, genomic imprinting, mRNA processing, and cell differentiation and development (Batista *et al.*). Dysregulation of lncRNAs is associated with various human diseases, including cancer. A growing number of dysregulated lncRNAs has been implicated in human carcinogenesis, including HOTAIR in breast cancer, MALAT-1 in lung cancer, HULC and HEIH in hepatocellular carcinoma, SPRY4-IT1 in melanoma, and PCGEM1 and ANRIL in prostate cancer (Gupta *et al.;* Ji *et al.;* Panzitt *et al.;* Yang *et al.;* Khaitan *et al.;* Petrovics *et al.;* Yap *et al.*). In addition, we recently analyzed two specific lncRNAs, HNF1A-AS1 and AFAP1-AS1, focusing on their involvement in the progression of BE into EAC (Yang, Song *et al.*; Wu, Bhagat *et al.*). Given the large number of lncRNA transcripts still remaining unstudied, we first sought to generate and analyze massively parallel RNA sequencing (RNAseq) data in order to identify and verify novel candidate lncRNAs that are dysregulated during neoplastic progression from NE to BE and finally to EAC.

MATERIALS AND METHODS

Cell lines and tissues

Primary, normal, non-immortalized esophageal epithelial cells (HEEpiC), along with the EAC cell lines FLO-1, SKGT4, and OE33, were purchased from ScienCell Research Laboratories (Carlsbad, California, USA), Sigma Chemical (St Louis, Missouri, USA), and the European Collection of Cell Culture (Porton Down, UK), respectively. The BE cell lines GiHTRT and QHTRT were generous gifts of Dr. Peter Rabinovitch, Fred Hutchinson Cancer Center, while JH-EsoAd1 EAC cells were generous gifts from Dr. James R. Eshleman. All media were supplemented with 10% fetal bovine serum (Invitrogen, San Diego, California, USA), unless otherwise stated.

Human tissues were obtained at endoscopy performed for clinical diagnostic indications and stored in liquid nitrogen prior to RNA extraction. All patients provided written informed consent under protocols approved by institutional review boards at the Johns Hopkins University School of Medicine, the University of Maryland School of Medicine, or the Baltimore Veterans Affairs Medical Center. All tissues were histopathologically confirmed as NE, BE, or EAC. Two matched sets of NE-BE-EAC tissues and two matched pairs of NE-BE tissues were studied by RNAseq. In addition, twenty-nine matched sets of NE-EAC tissues and fourteen matched pairs of NE-BE tissues were analyzed for differential expression of miR205HG.

RNA extraction and qRT-PCR

Total RNA was extracted using Trizol reagent (Invitrogen, Carlsbad, CA) and RNeasy kits (Qiagen, Valencia, CA), combined with RNase-free DNase (Qiagen, Valencia, CA). First-strand cDNA was synthesized from 500 ng of total RNA using a RevertAid™ cDNA synthesis kit (Fermentas, Glen Burnie, MD). qRT-PCR was performed using iQ SYBR Green Supermix on an iQ5 Multicolor Real-Time PCR Detection System (Bio-Rad, Hercules, CA). Gene expression levels were normalized to GAPDH expression and compared using the ddCt method. Two independent experiments were performed, each of which was carried out in triplicate. The sequences of all primers (Integrated DNA Technologies, Coralville, Iowa) are shown in Table 1.1. Total RNAs from normal tissues of 20 different organs were purchased from Applied Biosystems (Foster City, CA; Human total RNA survey panel kit). RNAs were stored at −80°C before and after analysis.

miRNA extraction and qRT-PCR

Total RNA was extracted using Trizol reagent (Invitrogen, Carlsbad, CA) and miRNeasy kit (Qiagen, Valencia, CA), combined with RNase-free DNase (Qiagen, Valencia, CA). cDNA was synthesized from 10 ng of total RNA using a TaqMan Reverse Transcription Kit (Applied Biosystems, Foster City, CA) and a specific primer from Taqman MicroRNA Assays (Applied Biosystems, Foster City, CA). qRT-PCR was performed using iQ Supermix (Bio-rad, Hercules, CA) and a labeled probe from Taqman MicroRNA Assays (Applied Biosystems, Foster City, CA). RNU6B small nuclear RNA was used as an internal control for normalization, and compared with the ddCt method.

Two independent experiments were performed, each of which was carried out in triplicate. RNAs were stored at −80°C before and after analysis.

Next-generation RNA sequencing

RNA was checked for quality using a BioAnalyzer, then depleted of rRNA using an Epicentre RiboZero kit. The remaining RNA (≤5%) was sheared using the Covaris system, then prepared as directional RNAseq libraries using the dUTP/UNG system. Paired-end 100 bp sequencing using an Illumina HiSeq 2000 was performed for each sample. Initial processing of data was done by the Illumina Sequence Control Software (SCS) and Pipeline 1.n software packages. These software components perform the functions of image analysis (Firecrest), base-calling (Bustard) and alignment of sequence tags to the Appropriate reference genome (ELAND), sorting samples by the index sequences (up to 4 per lane). For transcriptional profiling, to determine the relative counts of sequences from each gene relative to others, we obtained counts normalized by the total number of reads to allow inter-sample comparisons.

RESULTS

Next-generation RNA-seq analysis detects lncRNAs downregulated in BE and EAC

In order to identify novel tumor suppressor lncRNAs in Barrettogenesis and esophageal adenocarcinogenesis, we carried out RNA-seq of two NE-BE-EAC matched tissue sets and two NE-BE matched tissue pairs (full data available at GEO, Accession Number GSE48240). This RNA-seq analysis identified 1531 lncRNAs. Among these 1531

lncRNAs, we prioritized lncRNAs with the highest expression in NE (NE normalized copy number ≥ 10), which were sequentially downregulated during the NE-BE-EAC progression continuum (cut-off fold-change ≥ 1.5). This filtering process identified 11 lncRNAs (Table 1.2), among which CTA-55I10.1 (subsequently re-named to miR205HG) had the highest NE/BE and NE/EAC fold changes of these 11 candidate lncRNAs.

Significant miR205HG downregulation in BE and EAC primary tissues and cell lines are validated

We next proceeded to validate differential expression of the novel candidate lncRNA, miR205HG. Among ten alternatively spliced transcripts of this gene, transcripts with incomplete intron excision were excluded. Separate primer pairs were designed (data not shown) to distinguish between the different transcripts, and miR205HG-004 transcript (subsequently referred to as miR205HG) was chosen as the final candidate due to its showing the most robust expression level across all cell lines and tissues studied. miR205HG is a 908-nucleotide four-exon gene located at chromosomal band 1q32.2. Interestingly, the distal intron-exon junction between exons 3 and 4 harbors a miRNA-containing hairpin that serves as the template for two distinct miRNAs, miR-205 and miR-205* (Figure 1.1). According to the NCBI database, the miR-205 stem loop was shown to be more highly conserved than the overall miR205HG (data not shown).

qRT-PCR of miR205HG in Be and EAC cell lines versus primary NE (HEEpiC) cells revealed that miR205HG was either undetectable or greatly downregulated in both BE

(GiHTRT and QHTRT) cell lines and in all 4 EAC (FLO-1, JH-EsoAd1, OE33, and SKGT4) cell lines by 10-fold or greater (Figure 1.2). Expression of miR205HG's hosted miRNA, miR-205, showed a pattern similar to that of its host gene. Subsequently, matched NE-EAC tissue pairs from 29 EAC patients were tested for miR205HG expression by qRT-PCR. miR205HG expression was downregulated relative to NE in the vast majority of EACs studied (26/29, average fold-change 68.6, paired t-test p-value <0.0001; Figure 1.3) Similarly, when matched NE-BE tissue pairs from 14 patients with BE were tested for miR205HG expression by qRT-PCR, it was also downregulated relative to NE in all BEs studied (14/14, average fold-change 48.3, paired t-test p-value <0.0001; Figure 1.4) Both miR-205-5p and miR-205-3p were undetectable in all BE and EAC cell lines and tissues relative to the NE cell line or paired NE tissues (data not shown). Finally, we found that in addition to normal esophageal cell lines and tissues, miR205HG was widely expressed in normal cervix, prostate, trachea, and thymus (Figure 1.5).

DISCUSSION

During the past decade, the accuracy, speed, efficiency, and cost-effectiveness of deep sequencing have improved exponentially. Deep sequencing-based RNAseq provides a complete and highly quantitative assessment of all transcripts at single-nucleotide resolution. In this study, effective high-throughput expression analysis was applied to delineate unique lncRNA expression profiles at each stage of esophageal

adenocarcinogenesis. Since our previous study focused on oncogenic lncRNAs in EAC (Yang, Song *et al.*), we now sought to identify BE and EAC-suppressive lncRNAs.

Among 1531 lncRNAs identified by our initial RNAseq experiments, 11 tumor-suppressive lncRNAs were prioritized after a rigorous filtering process. By comparing normalized copy numbers from two matched sets of NE-BE-EAC tissues and two matched pairs of NE-BE tissues, our first project goal was to identify lncRNAs that were dysregulated early during Barrettogenesis, as well as later during eventual EAC tumorigenesis. In order to achieve this goal, we stipulated that candidate lncRNAs had to exhibit robust expression in NE (normalized copy number ≥ 10), and candidates also had to be sequentially downregulated at both the NE-BE and the BE-EAC progression steps (cut-off fold-change ≥ 1.5). miR205HG exhibited the greatest NE-BE and NE-BE-EAC fold-changes among our 11 filtered candidate lncRNAs.

In addition to analysis of our RNAseq data, Ensembl Genome Browser was used to further analyze this particular lncRNA. Interestingly, miR205HG is the host gene of a well-studied miRNA, miR-205, which has previously been shown to be significantly downregulated in both BE and EAC (Song *et al.*). As regards the host lncRNA, miR205HG has been studied as a pri-miR-205 in previous studies (Zhang *et al.*; Wu *et al.*), but none of these studies indicated that this lncRNA exerted its own independent function distinct from harboring miR-205. What makes this lncRNA structure intriguing is that miR-205 is located precisely within miR205HG's distal intron 3-exon 4 junction, so that when the host gene is spliced, the half of miR-205 hairpin is excised. Thus, the

miR-205 hairpin structure can only be processed while miR205HG is still in its pre-spliced form. We wondered why this evolutionarily conserved host gene had so many alternate splice forms if these other isoforms could not produce miR-205, reasoning that miR205HG must have independent biologic function(s) *distinct* from those of miR-205. Our hypothesis is not without precedent because H19, a well-studied cancer-related lncRNA, harbors miR-675 within one of its exons (Keniry *et al.*); similarly, lncRNA Dmn3os, which is crucial in embryonic skeletal formation, also harbors miR-199 and miR-214 within an exon (Watanabe *et al.*). However, it is also notable that these lncRNAs contain miRNAs completely within exons: knocking out or knocking down these lncRNAs simultaneously eliminates their hosted miRNAs. It is possible that these lncRNAs' biologic functions may have resulted merely from disruption of their hosted miRNAs. Unlike these other lncRNAs, our lncRNA allows us to excise miR-205 by eliminating one of miR205HG's introns, thereby facilitating efforts to study this lncRNA's independent functions.

Our qRT-PCR data validated our initial RNAseq discovery that miR205HG was significantly downregulated in both BE and EAC cells relative to NE cells, implying that dysregulation of miR205HG might drive early preneoplastic as well as later neoplastic transformation in the esophagus. Among 14 additional NE-BE tissue pairs tested, miR205HG was downregulated in all, with an average fold-change of 48.3 (p-value <0.0001); moreover, among 29 additional NE-EAC tissue pairs tested, miR205HG was downregulated in 89.7% of EAC tissues, with an average fold-change of 68.6 (p-value <0.0001). These impressively high average fold-change values and low p-values

underscored to us miR205HG's potential as a novel esophageal tumor suppressor gene. Moreover, with its expression pattern in normal cervix, prostate, trachea, and thymus, we reasoned that miR205HG could also exert important biological functions in these organs as well, where it could potentially contribute to diseases if dysregulated. We speculated that further studies in other tissue types, particularly miR205HG's effect on carcinogenesis, could offer further benefits to medical research, particularly if we could discover this intriguing lncRNA's biological function(s) in BE and EAC.

Finally, we also measured miR-205 expression level, which matched that of its host gene, hinting that both transcripts are coordinately controlled by the same promoter (miR-205* expression levels were negligible in a large variety of tissue types; data not shown). Thus, we then planned to study the relationship between these two transcripts as we discovered miR205HG's function(s) in BE and EAC. Overall, these promising qRT-PCR results encouraged our efforts to elucidate miR205HG's biological function(s).

CHAPTER TWO: STUDYING MIR205HG'S FUNCTION IN ESOPHAGEAL TUMORIGENESIS

INTRODUCTION

Elucidating a particular lncRNA's biological function(s) can be an extremely challenging and daunting task. Firstly, the enormous number of existing lncRNAs hinders any attempt at categorizing their functions when the majority of the population remains unstudied. Although current studies have identified a few categories of lncRNA function, additional functions are being proposed every day. Secondly, the lengths of lncRNAs also make it quite difficult to predict their functions. Unlike miRNAs, which span only 20-22 nts, lncRNAs are roughly defined as any transcript longer than 200 nts. Given the impact that each short miRNA strand has on its manifold target mRNAs, even the shortest lncRNAs could potentially perform diverse functions. Also, their greater length implies that lncRNAs may contain multiple regulatory elements permitting divergent functions to be active at different time points and in different contexts or tissues. Thus, considering even just these two aspects of lncRNAs, the number of combinations and permutations of imaginable lncRNA functions appears virtually unlimited.

Nonetheless, faced with such a novel lncRNA candidate, we found it helpful to review known functions of other lncRNAs. Current ongoing studies suggest that lncRNAs fulfill a wide variety of regulatory roles at almost every stage of gene expression. For example,

lncRNAs can regulate chromosomal structure *in cis* (XIST) or *in trans* (HOTAIR) (Clemson *et al.*; Gupta *et al.*). Other lncRNAs modulate the activity of protein-binding partners by acting as decoys to inhibit protein function (Martianov *et al.*; Kino *et al.*). Many lncRNAs are antisense to protein-coding genes and may function by regulating the splicing, editing, transport, translation, or degradation of their corresponding coding mRNA transcripts (Feng *et al.*; Bond *et al.*; Wang *et al.*). In addition, lncRNAs can be post-transcriptionally processed into short ncRNAs, which can in turn regulate gene expression (Franco-Zorrilla *et al.*; Poliseno *et al.*). With these known functions in mind, we sought to discover miR205HG's function(s) by performing several strategic functional studies.

MATERIALS AND METHODS

Generation of mir205HG-stable cell lines

A miR205HG insert was cloned into the pcDNA3.1(-) plasmid (Invitrogen, Carlsbad, CA). SKGT4 and FLO-1 EAC cells were seeded onto 6-well plates at a density of 1.5 x 10^5 cells/well. After 24 hours, 1 ug of a pcDNA3.1(-) plasmid either lacking an insert or containing a miR205HG insert was transfected using BioT transfection reagent (Bioland Scientific LLC, Paramount, CA), according to the manufacturer's protocol. After three weeks of selection in 600 ug/ml G418, several monoclonal colonies were selected per cell line and expanded. miR205HG expression levels were confirmed by qRT-PCR for each stable clone.

Cell proliferation assays

SKGT4 and FLO-1 miR205HG stably-transfected cells were re-seeded onto 96 well plates at a density of 1000 cells/well (Day 0). Cell proliferation was assessed at Day 1, Day 3, and Day 5, using the cell proliferation reagent WST-1 (Roche, Mannheim, Germany). 10 ul of reagent was added to each well, incubated at 37°C for 1 hour, and optical density was measured at 660 nm (background) and 440 nm (signal) using a plate reader (Molecular Devices, Sunnyvale, CA, USA). Independent experiments were repeated three times, with 6 replicates in each experiment.

Cell cycle analyses by flow cytometry

Flow cytometric analysis of DNA content was performed to assess cell cycle phase distribution. SKGT4 and FLO-1 miR205HG stable clones were incubated with PI staining buffer (PBS 0.1mg/mL PI, 0.6% NP40, 2mg/mL RNase A) for 30 min on ice (Roche Diagnostics, IN). DNA content was analyzed using a FACSCalibur (BD Biosciences, San Jose, CA) and Cell Quest software (BD Biosciences, MD) for histogram analysis.

Clonogenic assays

SKGT4 and FLO-1 miR205HG stably transfected cells were trypsinized into a single-cell suspension. A total of 100 cells were plated in each well of a 6-well plate and maintained for 14 days to allow colony formation. Clones containing more than 50 cells were counted using a grid. Three independent experiments were performed.

Injection of xenografted tumors in nude mice

All animal studies were approved by the Johns Hopkins Medical Institutes Animal Care Committee and were conducted in accordance with IACUC policy. A total of 15 female nude mice that were nine to ten weeks of age were obtained (Charles River, Boston) and divided into 3 groups (5 mice per group). FLO-1 miR205HG-stable cells were used to establish xenografted tumors. Control mice were injected with FLO-1 empty vector-only cells; the treatment group was injected with two different FLO-1 miR205HG-stable clones.

Each mouse was subcutaneously injected with 0.2 ml of tumor cells (2 x 10^6 cells) mixed in Matrigel into the left or right rear flank. After two weeks, mouse tumor volume was measured three times weekly. The width (W) and length (L) of each tumor were measured using a digital caliper and volume determined using the formula V = ½(L X W^2).

RESULTS

Overexpression of miR205HG inhibits EAC cell proliferation and colony formation

In order to observe miR205HG's effect on cell proliferation, we designed a pcDNA3.1-miR205HG construct lacking its wild-type intronic miR-205 hairpin structure. This design scheme enabled us to focus on the effect of overexpressed lncRNA without any

interference from miR-205. This construct was used to generate miR205HG-stable clones in two EAC cell lines, SKGT4 and FLO-1; qRT-PCR experiments confirmed miR205HG overexpression in both of these clones (Figure 2.1). These clones' miR205HG expression levels were not as high as in normal esophageal cells (data not shown), but significantly higher than vector-only clones.

Next, miR205HG-stable clones were used in WST-1 assays to detect the effect of miR205HG overexpression on proliferation of the EAC cell lines, SKGT4 and FLO-1. Compared to vector-only transfected negative control, forced overexpression of miR205HG decreased cell proliferation on Day 5 by 45% and 69% in SKGT4 and FLO-1 cells, respectively (p-values all <0.001; Figure 2.2). Colony size was also significantly smaller and relative colony number was reduced in FLO-1 and SKGT4 miR205HG-stable clones relative to control cells (Figure 2.3). Consistent with results of cell proliferation assays, clonogenic assays revealed that miR205HG overexpression caused a substantial reduction in colony formation in the SKGT4 (49% reduction; p-value <0.02) and FLO-1 (69% reduction; p-value <0.01) cell lines. These findings suggest that miR205HG suppresses EAC cell proliferation and their ability to undergo "unlimited" division, two known cancerous processes in epithelial cells.

Overexpression of miR205HG induces EAC G0-G1 cell cycle arrest

To delineate potential mechanisms underlying the growth-inhibitory effects of miR205HG overexpression, we assessed cell cycle progression in FLO-1 miR205HG-

stably transfected cells. Flow cytometric cell cycle assays demonstrated that relative to empty-vector transfected control cells, miR205HG overexpression led to an accumulation of cells at G0/G1-phase and a decrease in cells at S-phase (Figure 2.4). The proportion of apoptotic cells in the miR205HG-overexpressing vs. empty-vector negative control cell population were similar (data not shown). Thus, miR205HG-mediated inhibition of EAC cell proliferation and colony formation appeared to be mediated by modulation of the G1-S checkpoint, rather than by apoptosis.

miR205HG inhibits *in vivo* tumor growth

To evaluate whether miR205HG overexpression reduced esophageal tumor growth *in vivo*, we injected mice with FLO-1 stable cells lacking or containing a miR205HG insert. A total of 15 mice were evenly divided into 3 groups: mice were injected with either stable cells with no insert (control group) or with a miR205HG insert (treatment groups 1 and 2) in athymic nude mice and were observed for 36 days. Interestingly, treated animals began to show significantly smaller tumors on day 14 (control *vs.* treatment group 1, p-value =0.003; control *vs.* treatment group 2, p-value = 0.004); mean tumor volumes in treated groups 1 and 2 (37.1 ± 25.6 mm^3, 40.5 ± 20.5 mm^3, respectively) were significantly smaller than in the control group (83.4 ± 27.4 mm^3) (Figure 2.5). We continued to observe significant decreases in tumor growth in treated animals up to day 36 (control *vs.* treatment group 1, p-value =0.031; control *vs.* treatment group 2, p-value = 0.017); mean tumor volumes in treated groups 1 and 2 (140.9 ± 67.5 mm^3, 131.9 ± 44.1 mm^3, respectively) remained smaller than in control animals (231.0 ± 54.0 mm^3)

(Figure 2.5). This finding suggests that overexpressing miR205HG in EAC cells is sufficient to inhibit their *in vivo* growth.

We excised xenografts and H&E stained them for further histological analysis. Interestingly, while xenografts from vector-only controls were composed of densely packed sheets of cells with only occasional individual cell necrosis and leukocyte infiltration, xenografts from miR205HG-treated EAC cells showed clear signs of tumor cell loss, necrosis, leukocyte infiltration, and hemorrhage (Figure 2.6). As shown in this Figure, treated xenografts also contained areas of hemorrhage and necrosis (arrows), as well as leukocyte infiltration (miR205HG #1) or areas of tumor cell loss, accumulation of proteinaceous fluid, leukocyte infiltration and necrotic tumor cells (arrowheads) (miR205HG #2) (Table 1.3). These results demonstrate that forced miR205HG overexpression reduces EAC tumor growth by disrupting and killing tumor cells.

DISCUSSION

Most biological functions of lncRNAs remain obscure, and the involvement of lncRNAs in EAC pathogenesis and progression has not been widely studied. The current study permitted us to make a number of key observations concerning one particular lncRNA, miR205HG, in EAC. Firstly, we discovered that this previously unstudied lncRNA, when overexpressed, was capable of decreasing EAC cell growth, colony formation, and S-phase entry in multiple *in vitro* EAC models. Since the miR205HG-stable clones did not

manufacture any miR-205, this lncRNA was capable of independently exerting its tumor-suppressive effect, without any tumor-suppressive activity of its cognate miR Secondly, miR205HG overexpression inhibited *in vivo* tumor growth in athymic nude mice. Mean tumor size in the treatment groups was significantly smaller than in the control group throughout these experiments. Also, our histological analysis has revealed that miR205HG treated xenografts had more occurrences of tumor cell loss, necrosis, and hemorrhage. These results warrant further studies to develop novel therapeutic regimens leveraging miR205HG in the treatment of EAC.

Taken together, these findings suggest that miR205HG dysregulation contributes to the development and/or progression of EAC. The BE cell line and tissue qRT-PCR results in Chapter 1 illustrate that miR205HG dysregulation may also contribute to the neoplastic progression of BE. However, unfortunately, there is no clear BE animal model, and directly injecting BE cells into nude mice is not an option since these cells are not malignant. Nevertheless, we confirmed our novel lncRNA's tumor-suppressive function in EAC. The next step to determine its regulatory mechanisms will be even more challenging due to the diversity and complexity of mechanisms already known to underly lncRNA-mediated gene regulation. However, since miR205HG does not overlap or lie near any other coding genes, it may regulate remote genes *in trans* by modulating their protein partner(s). Also, although we have shown miR205HG to act independently of miR-205, the coordinate expression pattern of these two transcripts in various tissues suggests that this lncRNA may interact directly with its miRNA, or that the two RNAs

act synergistically. Thus, extrapolating from miR-205's known functions may provide clues to its host lncRNA's potential biologic function(s).

CHAPTER THREE: IDENTIFYING MIR205HG'S FUNCTION AS AN ESOPHAGEAL TUMOR-SUPPRESSIVE HEDGEHOG INHIBITOR

INTRODUCTION

Our previous experiments in Chapter 1 and 2 revealed that dysregulation of miR205HG may contribute to the neoplastic progression of BE, and that *in vitro* and *in vivo* overexpression of miR205HG inhibits EAC cell proliferation and tumor growth. In order to further elucidate miR205HG's mechanism of action and its specific downstream effectors, we investigated several well-studied pathways implicated in BE and EAC pathogenesis.

Aberrant activity of embryological signaling pathways has been implicated in the development of BE and EAC. Specifically, perturbations of the Hedgehog (HH), Bone Morphogenetic Protein (BMP), Wingless-Type MMTV Integration Site Family (WNT) and Retinoic acid (RA) signaling pathways have been observed in both BE and EAC. (Pavlov *et al.*) Among these pathways, HH signaling stands out for its importance in embryonic development of the gastrointestinal epithelium, including the esophageal epithelium, as well as its involvement in intestinal epithelial homeostasis.

By way of overview, the HH signaling pathway is involved in embryonic development, cell proliferation, tissue polarity, and carcinogenesis (Toftgard *et al.*; Hooper *et al.*;

Nusselein-Volhard *et al.*; Rubin *et al.*; Thayer *et al.*) Sonic Hedgehog (SHH), the best-studied ligand in the HH signaling pathway, binds to the membrane receptor Patched 1 homologue (PTCH1). PTCH1, in its resting inactive state, represses Smoothened (SMO), a G-protein coupled receptor; upon SHH-dependent activation of PTCH1, PTCH1 releases SMO. The activated SMO protein subsequently activates the GLI transcription factors, triggering further downstream signaling cascades.

Although SHH signaling is not active in normal adult esophageal cells, acid and bile reflux have been implicated in triggering abnormal activation of SHH signaling in the esophagus, thereby contributing to BE pathogenesis (Yang *et al.*). In support of this mechanism, SHH signaling was found to contribute to BE development by activating BMP signaling and inducing epithelial expression of SOX9, a transcription factor associated with intestinal stem cells (Wang *et al.*). As regards the development of frank EAC, upregulated SHH signaling is often observed in human EAC, and this enhanced signaling appears to stimulate EAC cell survival and proliferation *in vitro* (Wang *et al.*; Ma *et al.*; Yang *et al.*). In summary, the SHH signaling pathway appears to trigger both the origin of BE and its progression toward dysplasia and EAC, thus providing an attractive miR205HG-interacting target in the prevention of both premalignant BE and full-blown esophageal malignancy.

MATERIALS AND METHODS

Cell lines and tissues

Primary, normal, non-immortalized esophageal epithelial cells (HEEpiC), as well as the EAC cell lines FLO-1 and SKGT4 and the gastric cancer cell line AGS were purchased from ScienCell Research Laboratories (Carlsbad, California, USA) and Sigma Chemical (St Louis, Missouri, USA). The BE cell lines GiHTRT and QHTRT were generous gifts of Dr. Peter Rabinovitch, Fred Hutchinson Cancer Center. Please see the Methods Section in Chapter 1 for human tissue sample information.

RNA extraction and qRT-PCR

Total RNA was extracted using Trizol reagent (Invitrogen, Carlsbad, CA) and RNeasy kits (Qiagen, Valencia, CA), combined with RNase-free DNase (Qiagen, Valencia, CA). First-strand cDNA was synthesized from 500 ng of total RNA using a RevertAid™ cDNA synthesis kit (Fermentas, Glen Burnie, MD). qRT-PCR was performed using iQ SYBR Green Supermix on an iQ5 Multicolor Real-Time PCR Detection System (Bio-Rad, Hercules, CA). Gene expression levels were normalized to GAPDH expression and compared using the ddCt method. Two independent experiments were performed, each of which was carried out in triplicate. The sequences of all primers (Integrated DNA Technologies, Coralville, Iowa) are shown in Table 1.1.

miRNA extraction and qRT-PCR

Total RNA was extracted using Trizol reagent (Invitrogen, Carlsbad, CA) and miRNeasy kit (Qiagen, Valencia, CA), combined with RNase-free DNase (Qiagen, Valencia, CA). cDNA was synthesized from 10 ng of total RNA using a TaqMan Reverse Transcription Kit (Applied Biosystems, Foster City, CA) and a specific primer from Taqman

MicroRNA Assays (Applied Biosystems, Foster City, CA). qRT-PCR was performed using iQ Supermix (Bio-rad, Hercules, CA) and a labeled probe from Taqman MicroRNA Assays (Applied Biosystems, Foster City, CA). RNU6B small nuclear RNA was used as an internal control for normalization, and compared with the ddCt method. Two independent experiments were performed, each of which was carried out in triplicate. RNAs were stored at −80°C before and after analysis.

Transient transfection of mir205HG plasmid

A miR205HG insert was cloned into the pcDNA3.1(-) plasmid (Invitrogen, Carlsbad, CA). GiHTRT and QHTRT BE cells were seeded onto 6-well plates at a density of 1.5 x 10^5 cells/well. After 24 hours, 1~1.5 ug of a pcDNA3.1(-) plasmid either lacking an insert or containing a miR205HG insert was transfected using BioT transfection reagent (Bioland Scientific LLC, Paramount, CA), according to the manufacturer's protocol. GiHTRT cells were more sensitive to transfection reagent than QHTRT cells, so 1.0 ug of miR205HG plasmid was used for GiHTRT cells while 1.5 ug of miR205HG plasmid was used for QHTRT cells. Cells were harvested for RNA after 48 hr of transfection.

Transfection of miR mimics

Synthesized RNA duplexes of miR mimics were purchased from Dharmacon (Lafayette, CO). 50~70% confluent FLO-1 EAC cells were transfected with 50-60nM of mimic negative control or miR-205 mimic using Lipofectamine RNAiMAX (Invitrogen). RNA was harvested after 48 hours of transfection.

miRNA binding site prediction

Three different online miRNA target prediction engines (miRanda, Diana Tools 5.0: microT-CDS, and RNAhybrid 2.2) were used to predict miR-205 binding sites on PTCH1 3'UTR. Since no consensus was found among all three engines, each prediction result was considered with equal importance.

Luciferase reporter assays

The full-length PTCH1 3' untranslated region (3'UTR), containing several miR-205 predicted binding sites, was amplified from genomic DNA using linker primers containing *NheI* and *XhoI* restriction sites. Amplicons were cut and cloned into pmirGLO-dual luciferase vector just downstream of the firefly luciferase structural gene (Promega, Madison, WI). Similarly, three truncated PTCH1 3'UTRs were constructed and cloned into pmiRGLO-dual luciferase vector. An empty vector without PTCH1 3'UTR was used as a negative control for these assays.

FLO-1 cells were seeded onto 96-well plates two days prior to dual-luciferase vector transfection, then transfected with miR-205 mimic. AGS cells were plated the day before the dual-luciferase vector transfection. The constructed pmirGLO-PTCH1 vectors were transfected into both FLO-1 (24 h after miR mimic transfection) and AGS cells using BioT transfection reagent (Bioland Scientific LLC, Paramount, CA). 24 hours after dual-

luciferase vector transfection, luciferase reporter assays were performed using a Dual-Glo luciferase assay kit (Promega). Luminescence intensity was measured by VICTOR2 fluorometry (Perkin Elmer, Waltham, MA), and the luminescence intensity of Firefly luciferase was normalized to that of Renilla luciferase.

Western Blotting

Cells were lysed in 100 μl of cell lysis buffer (NaCl: 149mM, Nonidet P-40: 0.01%, Tris: 50 mM, pH 7.8, and protease inhibitor cocktail: 0.5% (Sigma, Saint Louis, MO). Protein concentration was determined using a BCA Protein Assay Kit (Pierce, Rockford, IL) with human serum albumin as a standard. 30 ug of each sample was loaded into one well of a 10%TRIS-HCL electrophoretic gel (Bio Rad, Hercules, CA). After electrophoresis, protein was transferred onto a PVDF membrane (Millipore corp, Bedford, MA). The membranes were immunoblotted with TBS containing 5% nonfat dry milk, washed with 0.1% TBST, and probed with 1:1000 anti-SHH rabbit monoclonal antibody (Cat# 8358S, Cell Signaling, Danvers, MA) and 1:7000 anti-human β-actin rabbit monoclonal antibody (Cat# A5060, Sigma-Aldrich, Bedford, MA, USA). Horseradish peroxidase-conjugated anti-rabbit goat IgG (1:3000) (Calbiochem, Cat# 401393, San Diego, CA) and an ECL Western Blotting detection kit (Amersham Pharmacia Biotech, Piscataway, NJ) were used for the target protein visualization.

Statistical analysis

Statistical analysis was performed using GraphPad Prism 6.04 software (GraphPad, La Jolla, CA). Experimental results were evaluated using the two-tailed Student's t-test or Spearman rank correlation test. All values were expressed as mean±SD. Statistical significance was noted at p-value <0.05, and three independent triplicate experiments were performed for cell biological assays, unless otherwise stated.

RESULTS

Key SHH signaling genes are upregulated in BE and EAC cell lines, and miR205HG and SHH expression levels are inversely correlated in BE and EAC matched tissues

qRT-PCR of BE and EAC cell lines versus primary NE (HEEpiC) cells revealed that relative to NE cells, RNA expression levels of the key SHH pathway genes SHH, PTCH1, SMO, and GLI1 were upregulated in both BE cell lines and in all 4 EAC cell lines (Figure 3.1). Interestingly, among the SHH pathway genes studied, the average expression fold-change in BE and EAC cells was greatest for SHH (average fold-change 45.2 and 1,029, respectively) and GLI1 (average fold-change 1,296 and 1,539, respectively). These results agree with previous studies reporting upregulated expression of SHH signaling genes in BE and EAC (Yang *et al.*; Wang *et al.*).

The same matched NE-EAC tissue pairs from 26 EAC patients (not 29 because 3 paired tissue RNAs were depleted) that had already been tested for miR205HG expression were also tested for SHH expression by qRT-PCR. SHH expression was upregulated relative to

NE in the majority of EACs studied (23/26, average fold-change 154.7, paired t-test p-value <0.0001; Figure 3.2) Similarly, when matched NE-BE tissue pairs from 14 patients with BE were tested by qRT-PCR, SHH was also upregulated relative to NE in all BEs studied (14/14, average fold-change 2,913.0, paired t-test p-value <0.0001; Figure 3.3) Interestingly, in both matched BE and EAC tissues, miR205HG and SHH expression levels were inversely correlated (r = -0.73, p-value = 0.0001; r = -0.83, p-value = 0.0004, respectively) (Figure 3.2, Figure 3.3). It was not surprising to find SHH upregulation in patient tissues, but this strong inverse correlation between miR205HG and SHH was highly encouraging and interesting. Since SHH upregulation and miR205HG downregulation are both implicated in driving the genesis and progression of BE and EAC, we speculated that miR205HG directly or indirectly inhibits SHH transcription in NE cells. We utilized miR205HG-inserted plasmids to further test this theory.

SHH downregulation in miR205HG-transfected EAC clones

miR205HG-stable EAC clones were used to assess the effect, if any, of forced miR205HG overexpression on key SHH signaling genes. Relative to vector-only transfected negative control, qRT-PCR results from miR205HG-stable EAC clones showed significant reductions in SHH, PTCH1, SMO, and GLI1 expression levels (Figure 3.4). We also performed Western blots, which demonstrated that SHH protein levels were greatly reduced in SKGT4 and FLO-1 miR205HG-stable clones (Figure 3.5). PTCH1, SMO and GLI1 protein levels did not change with forced miR205HG overexpression (data not shown). The lack of change in these protein levels could have resulted from an antibody sensitivity issue or a negligible impact of miR205HG on

protein translation. Nevertheless, we have established that miR205HG targets SHH and reduces its RNA and protein levels. This lncRNA's ability to inhibit SHH may have important consequences in disrupting signaling.

miR-205 directly binds to the PTCH1 3'UTR

We had previously considered the possibility that miR-205 could act as its own host gene's synergistic partner. We therefore looked for further potential synergistic roles of these two closely related transcripts. Specifically, after discovering that miR205HG was implicated in the SHH signaling pathway, we examined whether miR-205 could also target this same pathway. We transfected FLO-1 EAC cells with a negative control mimic or a miR-205 mimic, and harvested RNA to perform qRT-PCR. Among four genes tested (SHH, PTCH1, SMO, GLI1), only PTCH1 showed a significant (p-value = 0.0001) reduction when transfected with 60 nM of miR-205 mimic (Figure 3.6). In order to assess direct binding of miR-205 to the 3'UTR of PTCH1, we constructed various luciferase vectors. Three different online miRNA target prediction engines (miRanda, Diana Tools 5.0: microT-CDS, and RNAhybrid 2.2) were used to predict miR-205 binding sites on the PTCH1 3'UTR. Since no consensus could be found among the three engines, all 11 binding predictions were considered equally. Since it would have been inefficient and time-consuming to mutagenize all 11 sites, we decided to narrow down the predicted miR-205 binding sites by constructing three different truncated versions of the PTCH1 3'UTR (Figure 3.7).

Luciferase assays were performed using FLO-1 EAC cells transfected with miR-205 mimic. At the same time, we also used AGS gastric adenocarcinoma cell lines, because this cell line expresses high levels of both miR205HG and miR-205 (data not shown) - thus removing the need to transfect a synthetic miR-205 mimic construct. AGS cells were substituted for NE cells because HEEpiC primary cells are not robust enough to survive luciferase assays. Next, mimic-transfected FLO-1 or AGS cells were transfected with a pmiRGLO-full length PTCH1 3'UTR vector or pmiRGLO-truncated versions of the PTCH1 3'UTR vectors. Relative to luciferase activity detected after pmiRGLO vector-only transfection, the full-length 3'UTR insert caused the most significant reduction of luciferase activity in both FLO-1 and AGS cells (Figure 3.8). This result confirmed that miR-205, like its host gene miR205HG, also targets the SHH signaling pathway, in this case by directly binding and downregulating PTCH1.

DISCUSSION

We confirmed the finding that several key SHH signaling genes are upregulated in BE and EAC cells, as expected. More importantly, we discovered that miR205HG and SHH correlate inversely in matched patient tissue samples. Our follow-up experiments revealed that overexpression of miR205HG inhibits the transcription and translation of SHH itself, as well as the transcription of the SHH pathway genes PTCH1, SMO and GLI1. While this result is quite encouraging, it also generates additional questions. Firstly, we do not know exactly how miR205HG overexpression leads to SHH inhibition. It is possible that miR205HG interacts directly with the SHH promoter, thereby preventing

transcription factors from binding and initiating SHH transcription. Another possibility is that miR205HG interacts with Polycomb Repressive Complex 2 (PRC2) and regulates the chromatin state in the vicinity of the SHH gene. Future experiments are needed to elucidate miR205HG's specific mechanism(s) of action. Secondly, although SHH and several key SHH signaling genes are downregulated by miR205HG, we have no direct proof that the entire SHH signaling pathway is inhibited by our lncRNA. We can argue that SHH signaling is probably inhibited, based on our finding that miR205HG overexpression reduces cell proliferation, clonogenicity, and *in vivo* tumor growth: these results resemble previously reported phenotypes of SHH signaling inhibition in cancer cells. However, if we employ a Gli reporter construct to measure SHH signaling activity in miR205HG-stably transected cells, it may provide stronger direct evidence that miR205HG targets SHH and shuts down the entire signaling pathway.

We also explored miR-205 and its potential synergistic role with miR205HG in the SHH pathway. Our luciferase assay data established that miR-205 directly binds to and downregulates PTCH1. Since the PTCH1 receptor inhibits SMO, miR-205-induced downregulation of PTCH1 would be expected to result in activation of SMO. This data contradicts our initial prediction that miR205HG and miR-205 act synergistically, with miR205HG inhibiting SHH. One plausible explanation for this conundrum is the possibility that miR-205 is involved in a negative feedback loop in response to downregulation of SHH by miR205HG. Another alternative explanation is that these two transcripts do not in fact act synergistically. However, one recent study also reported PTCH1 expression in 58% of BE and 96% of EAC lesions (Yang *et al.*). Notably, our

data herein establish that PTCH1 is upregulated in BE and EAC cell lines, and that forced miR205HG overexpression reduces PTCH1 expression in EAC cells. Based on this evidence, miR205HG and mir-205 may still act synergistically. Thus, the precise mechanisms of action of the lncRNA miR205HG await full elucidation, with attendant complexities and nuances.

SUMMARY

This project was initiated to study a previously uncharacterized lncRNA, without full comprehension of directions in which this study might lead. The only directional clue we had at the outset was our finding that this lncRNA was downregulated in the majority of BE and EAC cells and tissues relative to NE cells and tissues. We also knew that this lncRNA hosted a well-studied miRNA. From these limited clues, we designed various functional *in vitro* and *in vivo* experiments to elucidate our lncRNA's biologic functions and its specific mechanisms of action. Our data established that miR205HG is dysregulated early during neoplastic progression from NE to BE and eventually to EAC; this dysregulation may result in abnormally upregulated SHH transcription and translation, wherein the increased availability of this pathway ligand triggers the downstream HH signaling cascade. Although miR-205's specific involvement in miR205HG is still unclear, miR-205 also appears to influence the HH pathway by targeting and downregulating PTCH1. It was fascinating to discover that what previously seemed to be merely a miRNA host gene actually possessed independent functional activity, capable of critically altering esophageal cell fate and behavior. Our results thus highlight the broader importance of miRNA host gene lncRNAs and their potential functions. We analyzed the NCBI GenBank and MiRBase databases to assess how many lncRNA host genes were contained in the human genome. This analysis revealed 158 lncRNAs containing in total 154 miRNAs. This finding suggests a plethora of lncRNA host genes in need of study: such studies will likely generate further novel insights into how lncRNAs interact with their host miRNAs in particular, and into the functions of all

lncRNAs in general. In view of the rapidly burgeoning evidence of the importance of lncRNAs, such insights could prove paradigm-shifting not only in cancer biology and cancer medicine in particular, but in all biology and all diseases in general.

REFERENCES

Batista, P. J., & Chang, H. Y. (2013). Long noncoding RNAs: cellular address codes in development and disease. *Cell, 152*(6), 1298-1307.

Cameron, A. J. (1998). Management of Barrett's esophagus. *Mayo Clin Proc, 73*(5), 457-461.

Cesana, M., Cacchiarelli, D., Legnini, I., Santini, T., Sthandier, O., Chinappi, M., . . . Bozzoni, I. (2011). A long noncoding RNA controls muscle differentiation by functioning as a competing endogenous RNA. *Cell, 147*(2), 358-369.

Clemson, C. M., McNeil, J. A., Willard, H. F., & Lawrence, J. B. (1996). XIST RNA paints the inactive X chromosome at interphase: evidence for a novel RNA involved in nuclear/chromosome structure. *J Cell Biol, 132*(3), 259-275.

Corley, D. A., Levin, T. R., Habel, L. A., Weiss, N. S., & Buffler, P. A. (2002). Surveillance and survival in Barrett's adenocarcinomas: a population-based study. *Gastroenterology, 122*(3), 633-640.

Enzinger, P. C., & Mayer, R. J. (2003). Esophageal cancer. *N Engl J Med, 349*(23), 2241-2252.

Franco-Zorrilla, J. M., Valli, A., Todesco, M., Mateos, I., Puga, M. I., Rubio-Somoza, I., . . . Paz-Ares, J. (2007). Target mimicry provides a new mechanism for regulation of microRNA activity. *Nat Genet, 39*(8), 1033-1037.

Gilbert, E. W., Luna, R. A., Harrison, V. L., & Hunter, J. G. (2011). Barrett's esophagus: a review of the literature. *J Gastrointest Surg, 15*(5), 708-718.

Gupta, R. A., Shah, N., Wang, K. C., Kim, J., Horlings, H. M., Wong, D. J., . . . Chang, H. Y. (2010). Long non-coding RNA HOTAIR reprograms chromatin state to promote cancer metastasis. *Nature, 464*(7291), 1071-1076.

Hooper, J. E., & Scott, M. P. (2005). Communicating with Hedgehogs. *Nat Rev Mol Cell Biol, 6*(4), 306-317.

Ji, P., Diederichs, S., Wang, W., Boing, S., Metzger, R., Schneider, P. M., . . . Muller-Tidow, C. (2003). MALAT-1, a novel noncoding RNA, and thymosin beta4 predict metastasis and survival in early-stage non-small cell lung cancer. *Oncogene, 22*(39), 8031-8041.

Keniry, A., Oxley, D., Monnier, P., Kyba, M., Dandolo, L., Smits, G., & Reik, W. (2012). The H19 lincRNA is a developmental reservoir of miR-675 that suppresses growth and Igf1r. *Nat Cell Biol, 14*(7), 659-665.

Khaitan, D., Dinger, M. E., Mazar, J., Crawford, J., Smith, M. A., Mattick, J. S., & Perera, R. J. (2011). The melanoma-upregulated long noncoding RNA SPRY4-IT1 modulates apoptosis and invasion. *Cancer Res, 71*(11), 3852-3862.

Kino, T., Hurt, D. E., Ichijo, T., Nader, N., & Chrousos, G. P. (2010). Noncoding RNA gas5 is a growth arrest- and starvation-associated repressor of the glucocorticoid receptor. *Sci Signal, 3*(107), ra8.

Ma, X., Sheng, T., Zhang, Y., Zhang, X., He, J., Huang, S., . . . Xie, J. (2006). Hedgehog signaling is activated in subsets of esophageal cancers. *Int J Cancer, 118*(1), 139-148.

Martianov, I., Ramadass, A., Serra Barros, A., Chow, N., & Akoulitchev, A. (2007). Repression of the human dihydrofolate reductase gene by a non-coding interfering transcript. *Nature, 445*(7128), 666-670.

Nie, L., Wu, H. J., Hsu, J. M., Chang, S. S., Labaff, A. M., Li, C. W., . . . Hung, M. C. (2012). Long non-coding RNAs: versatile master regulators of gene expression and crucial players in cancer. *Am J Transl Res, 4*(2), 127-150.

Nusslein-Volhard, C., & Wieschaus, E. (1980). Mutations affecting segment number and polarity in Drosophila. *Nature, 287*(5785), 795-801.

Panzitt, K., Tschernatsch, M. M., Guelly, C., Moustafa, T., Stradner, M., Strohmaier, H. M., . . . Zatloukal, K. (2007). Characterization of HULC, a novel gene with striking up-regulation in hepatocellular carcinoma, as noncoding RNA. *Gastroenterology, 132*(1), 330-342.

Petrovics, G., Zhang, W., Makarem, M., Street, J. P., Connelly, R., Sun, L., . . . Srivastava, S. (2004). Elevated expression of PCGEM1, a prostate-specific gene with cell growth-promoting function, is associated with high-risk prostate cancer patients. *Oncogene, 23*(2), 605-611.

Poliseno, L., Salmena, L., Zhang, J., Carver, B., Haveman, W. J., & Pandolfi, P. P. (2010). A coding-independent function of gene and pseudogene mRNAs regulates tumour biology. *Nature,*

465(7301), 1033-1038.
Rubin, L. L., & de Sauvage, F. J. (2006). Targeting the Hedgehog pathway in cancer. *Nat Rev Drug Discov, 5*(12), 1026-1033.
Schneider, J. L., & Corley, D. A. (2015). A review of the epidemiology of Barrett's oesophagus and oesophageal adenocarcinoma. *Best Pract Res Clin Gastroenterol, 29*(1), 29-39.
Sharma, P., Falk, G. W., Weston, A. P., Reker, D., Johnston, M., & Sampliner, R. E. (2006). Dysplasia and cancer in a large multicenter cohort of patients with Barrett's esophagus. *Clin Gastroenterol Hepatol, 4*(5), 566-572.
Song, J. H., & Meltzer, S. J. (2012). MicroRNAs in pathogenesis, diagnosis, and treatment of gastroesophageal cancers. *Gastroenterology, 143*(1), 35-47 e32.
Thayer, S. P., di Magliano, M. P., Heiser, P. W., Nielsen, C. M., Roberts, D. J., Lauwers, G. Y., . . . Hebrok, M. (2003). Hedgehog is an early and late mediator of pancreatic cancer tumorigenesis. *Nature, 425*(6960), 851-856.
Toftgard, R. (2000). Hedgehog signalling in cancer. *Cell Mol Life Sci, 57*(12), 1720-1731.
van Soest, E. M., Dieleman, J. P., Siersema, P. D., Sturkenboom, M. C., & Kuipers, E. J. (2005). Increasing incidence of Barrett's oesophagus in the general population. *Gut, 54*(8), 1062-1066.
Walsh, A. L., Tuzova, A. V., Bolton, E. M., Lynch, T. H., & Perry, A. S. (2014). Long noncoding RNAs and prostate carcinogenesis: the missing 'linc'? *Trends Mol Med, 20*(8), 428-436.
Wang, D. H., Clemons, N. J., Miyashita, T., Dupuy, A. J., Zhang, W., Szczepny, A., . . . Watkins, D. N. (2010). Aberrant epithelial-mesenchymal Hedgehog signaling characterizes Barrett's metaplasia. *Gastroenterology, 138*(5), 1810-1822.
Wang, X., Arai, S., Song, X., Reichart, D., Du, K., Pascual, G., . . . Kurokawa, R. (2008). Induced ncRNAs allosterically modify RNA-binding proteins in cis to inhibit transcription. *Nature, 454*(7200), 126-130.
Watanabe, T., Sato, T., Amano, T., Kawamura, Y., Kawamura, N., Kawaguchi, H., . . . Nakaoka, T. (2008). Dnm3os, a non-coding RNA, is required for normal growth and skeletal development in mice. *Dev Dyn, 237*(12), 3738-3748.
Wu, H., & Mo, Y. Y. (2009). Targeting miR-205 in breast cancer. *Expert Opin Ther Targets, 13*(12), 1439-1448.
Wu, W., Bhagat, T. D., Yang, X., Song, J. H., Cheng, Y., Agarwal, R., . . . Meltzer, S. J. (2013). Hypomethylation of noncoding DNA regions and overexpression of the long noncoding RNA, AFAP1-AS1, in Barrett's esophagus and esophageal adenocarcinoma. *Gastroenterology, 144*(5), 956-966 e954.
Yang, F., Zhang, L., Huo, X. S., Yuan, J. H., Xu, D., Yuan, S. X., . . . Sun, S. H. (2011). Long noncoding RNA high expression in hepatocellular carcinoma facilitates tumor growth through enhancer of zeste homolog 2 in humans. *Hepatology, 54*(5), 1679-1689.
Yang, L., Wang, L. S., Chen, X. L., Gatalica, Z., Qiu, S., Liu, Z., . . . Xie, J. (2012). Hedgehog signaling activation in the development of squamous cell carcinoma and adenocarcinoma of esophagus. *Int J Biochem Mol Biol, 3*(1), 46-57.
Yang, X., Song, J. H., Cheng, Y., Wu, W., Bhagat, T., Yu, Y., . . . Mori, Y. (2014). Long non-coding RNA HNF1A-AS1 regulates proliferation and migration in oesophageal adenocarcinoma cells. *Gut, 63*(6), 881-890.
Yap, K. L., Li, S., Munoz-Cabello, A. M., Raguz, S., Zeng, L., Mujtaba, S., . . . Zhou, M. M. (2010). Molecular interplay of the noncoding RNA ANRIL and methylated histone H3 lysine 27 by polycomb CBX7 in transcriptional silencing of INK4a. *Mol Cell, 38*(5), 662-674.
Zhang, T., Zhang, J., Cui, M., Liu, F., You, X., Du, Y., . . . Zhang, X. (2013). Hepatitis B virus X protein inhibits tumor suppressor miR-205 through inducing hypermethylation of miR-205 promoter to enhance carcinogenesis. *Neoplasia, 15*(11), 1282-1291.

TABLES

Table 1.1

Target Gene	Primer Direction	Sequence
miR205HG	Forward	GTGCTTTATATAGGAAAGGACCAAC
	Reverse	CCATGCCTCCTGAACTTCACT
SHH	Forward	GCTCGGTGAAAGCAGAGAAC
	Reverse	CCAGGAAAGTGAGGAAGTCG
PTCH1	Forward	TCCCAGCGCTTTCTACATCT
	Reverse	CTTTGTCGTGGACCCATTCT
GLI1	Forward	GTGCAAGTCAAGCCAGAACA
	Reverse	ATAGGGGCCTGACTGGAGAT
SMO	Forward	GTTCTCCATCAAGAGCAACCAC
	Reverse	CGATTCTTGATCTCACAGTCAGG

Sequences of forward and reverse primers used for qRT-PCR.

Table 1.2

Gene Information		Normalized Copy Numbers										Fold Change			
Accession	Name	NE1	BE1	EAC1	NE2	BE2	EAC2	NE3	BE3	NE4	BE4	NE/BE	NE/EAC	NE/BE	NE/EAC
ENSG00000230937	CTA-55I10.1	1,120	11	0	49	0	0	749	157	548	94	101.82	#DIV/0!	4.77	5.83
ENSG00000245460	AC079305.1	270	8	60	11	17	3	76	13	52	16	33.75	4.50	5.85	3.25
ENSG00000245532	NEAT1	41,741	3,557	12,330	11,208	29,426	8,631	47,273	12,815	32,335	8,864	11.73	3.39	3.69	3.65
ENSG00000228794	RP11-206L10.11	20	3	7	10	42	22	28	14	38	25	6.67	2.86	2.00	1.52
ENSG00000245937	CTC-228N24.3	99	6	38	16	34	8	34	27	32	10	16.50	2.61	1.26	3.20
ENSG00000177410	NCRNA00275	664	28	294	15	38	3	120	44	88	28	23.71	2.26	2.73	3.14
ENSG00000197989	SNHG12	240	33	113	13	11	5	49	24	53	18	7.27	2.12	2.04	2.94
ENSG00000203875	SNHG5	1,294	116	668	19	107	22	218	69	137	36	11.16	1.94	3.16	3.81
ENSG00000255717	SNHG1	4,665	657	2,426	22	37	15	126	29	96	25	7.10	1.92	4.34	3.84
ENSG00000219481	NBPF1	128	14	70	22	45	18	60	22	37	22	9.14	1.83	2.73	1.68
ENSG00000247828	CTC-358I24.1	70	4	41	10	49	15	54	25	55	26	17.50	1.71	2.16	2.12
ENSG00000234741	GAS5	3,907	459	2,302	30	64	17	219	90	160	66	8.51	1.70	2.43	2.42

RNAseq-generated normalized copy numbers of two matched NE-BE-EAC paired tissues and two matched NE-BE paired tissues are shown above (NE: Normal esophagus, BE: Barrett's esophagus, EAC: Esophageal adenocarcinoma). Top 11 tumor-suppressive lncRNA candidates are sorted by the highest NE/EAC fold change. We prioritized lncRNAs with the highest expression in NE (NE normalized copy number ≥ 10), which were sequentially downregulated during the NE-BE-EAC progression continuum (cut-off fold-change ≥ 1.5). Among 11 lncRNAs shown above, CTA-55I10.1 (subsequently re-named to miR205HG) had the highest NE/BE and NE/EAC fold changes.

Table 1.3

	Necrosis Score	Hem Score	Leuk Score	Total Score	Grade
Treatment Group #1 (L)	2	1	2	5	**2**
Treatment Group #1 (R)	2	3	1	6	**2**
Treatment Group #2 (L)	3	1	2	6	**2**
Treatment Group #2 (R)	3	2	2	7	**3**
Control (L)	1	0	1	2	**1**
Control (R)	1	1	1	3	**1**

A semi-quantitative histologic grading illustrates differences between vector-only xenograft controls and two miR205HG-treated EAC treatment groups (Necrosis: 0 = no tumor, 1 = <5% necrosis, 2 = 5-25% necrosis, 3 = > 25% necrosis; Hemorrhage: 0 = none, 1 = mild, 2 = moderate, 3 = marked; Leukocyte infiltration: 1 = mild occasional infiltrating cells, 2 = moderate multifocal clusters of infiltrates, 3 = severe, widespread and densely packed infiltrates). The final grade is the sum of the necrosis, hemorrhage, and leukocyte infiltration scores (grade 0 = total score 0; grade 1 = total score 1-3; grade 2 = total score 3-6; grade 3 = total score 7-9).

FIGURES

Figure 1.1

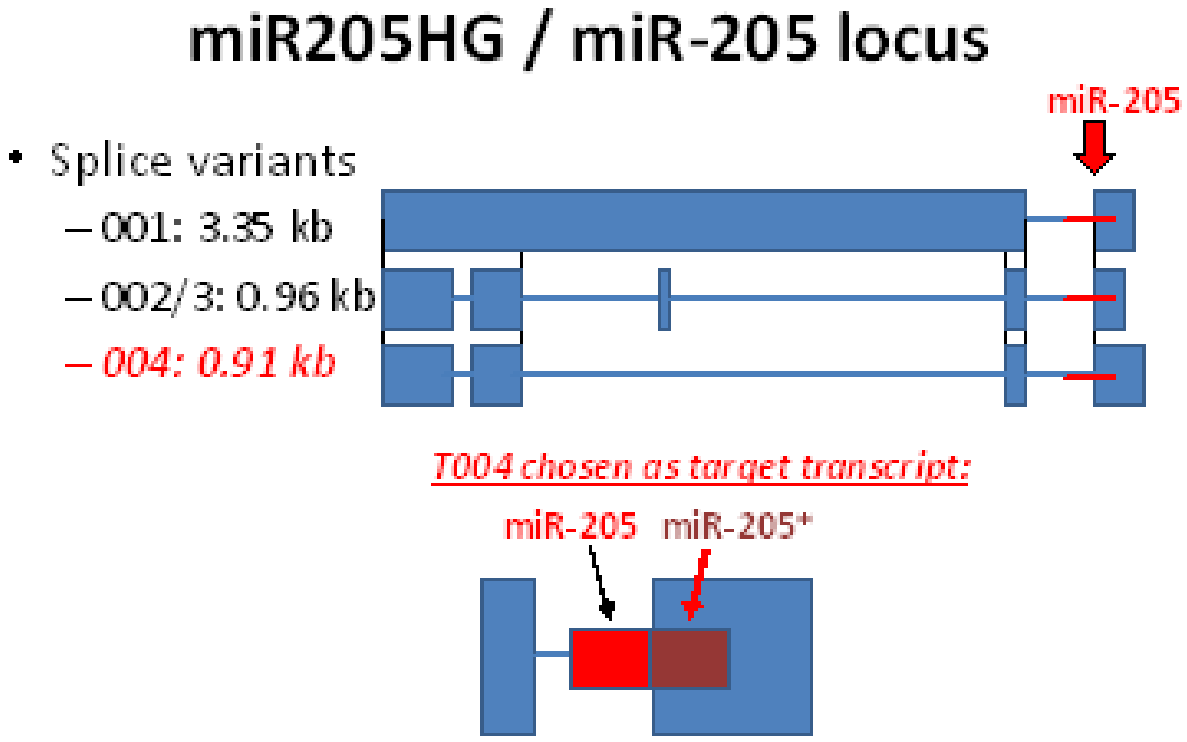

Illustration of miR205HG gene locus is presented with 3 of its transcript variants and their transcript sizes (kb). miR-205 location is highlighted in its location in miR205HG's exon-intron junction.

Figure 1.2

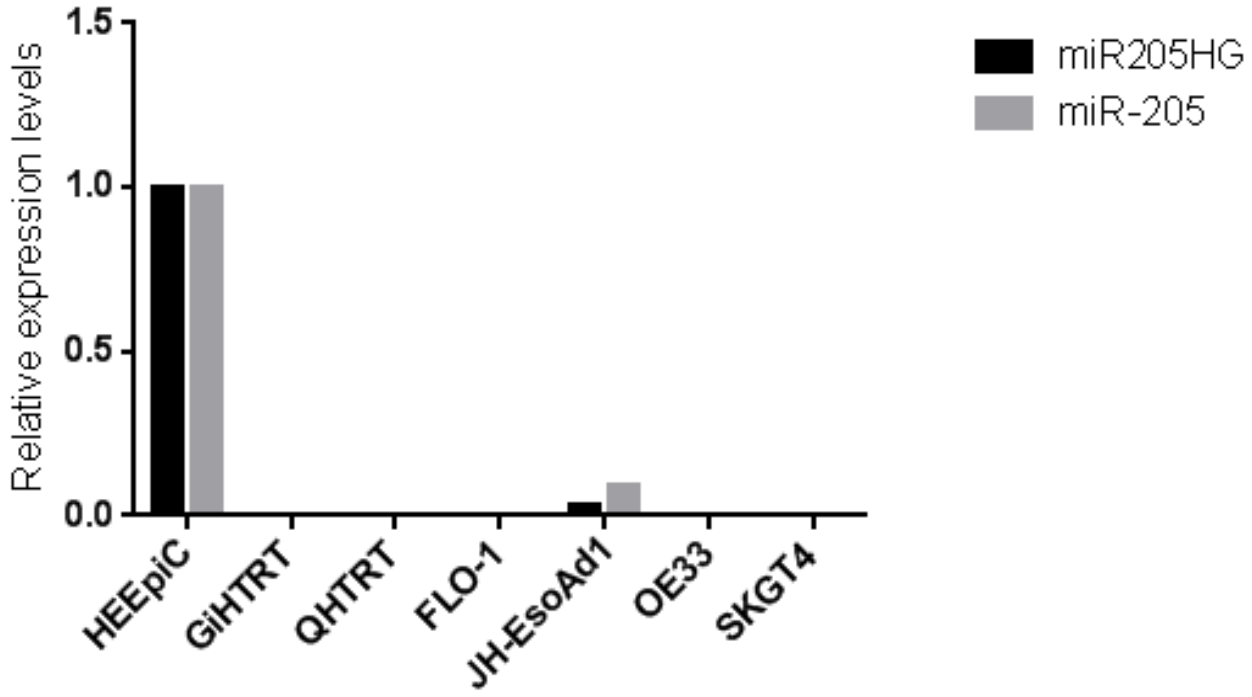

qRT-PCR expression levels of miR205HG and miR-205 in BE (GiHTRT and QHTRT) and EAC (OE33, Flo-1, SKGT4, and JH-ea1) cell lines relative to NE (HEEPiC) cells. Both miR205HG and miR-205 were either not detectable or greatly downregulated by 10-fold or greater.

Figure 1.3

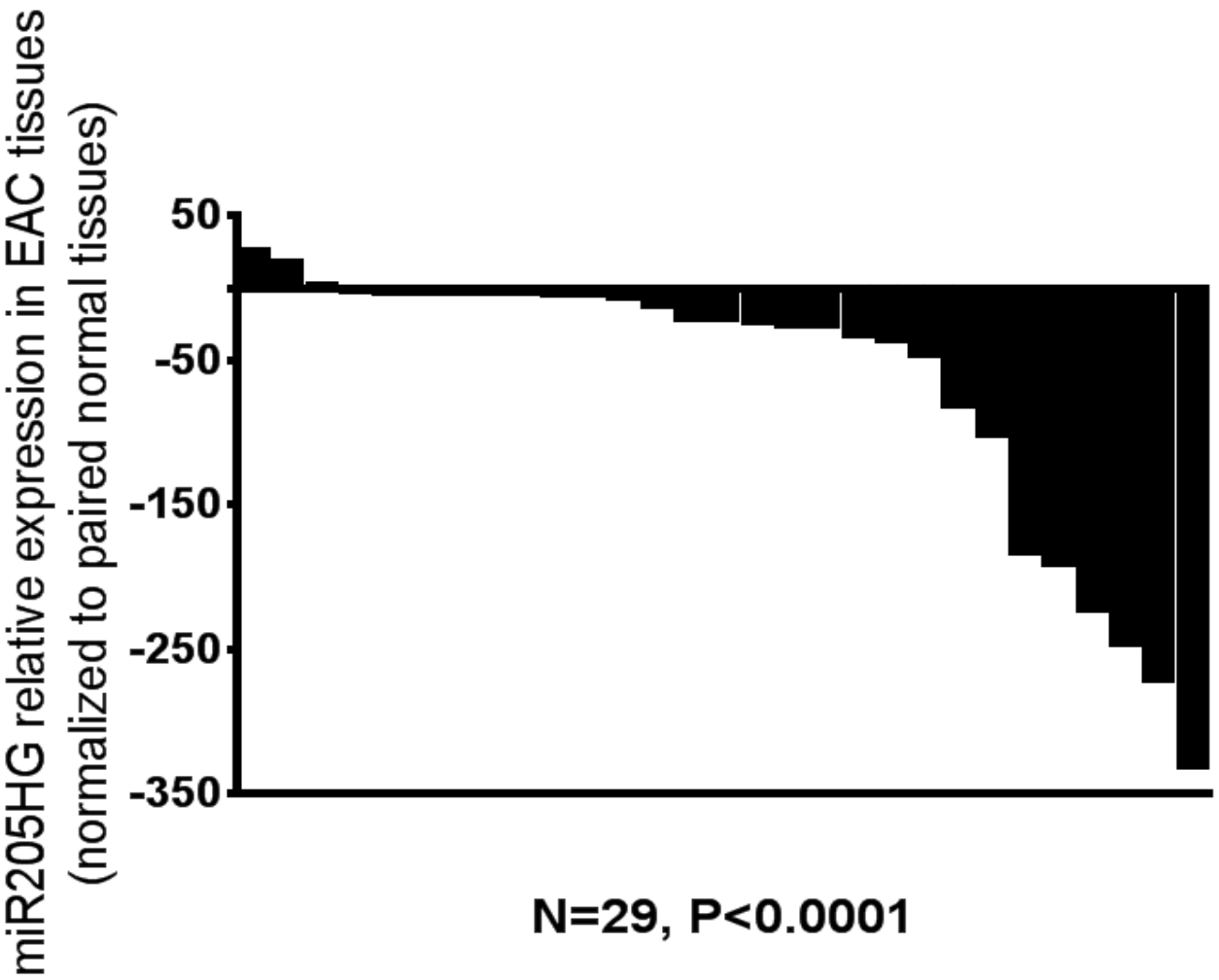

29 matched NE-EAC tissue pairs were tested for miR205HG expression by qRT-PCR. miR205HG expression was downregulated relative to NE in the vast majority of EACs studied (26/29, average fold-change 68.6, paired t-test p-value <0.0001).

Figure 1.4

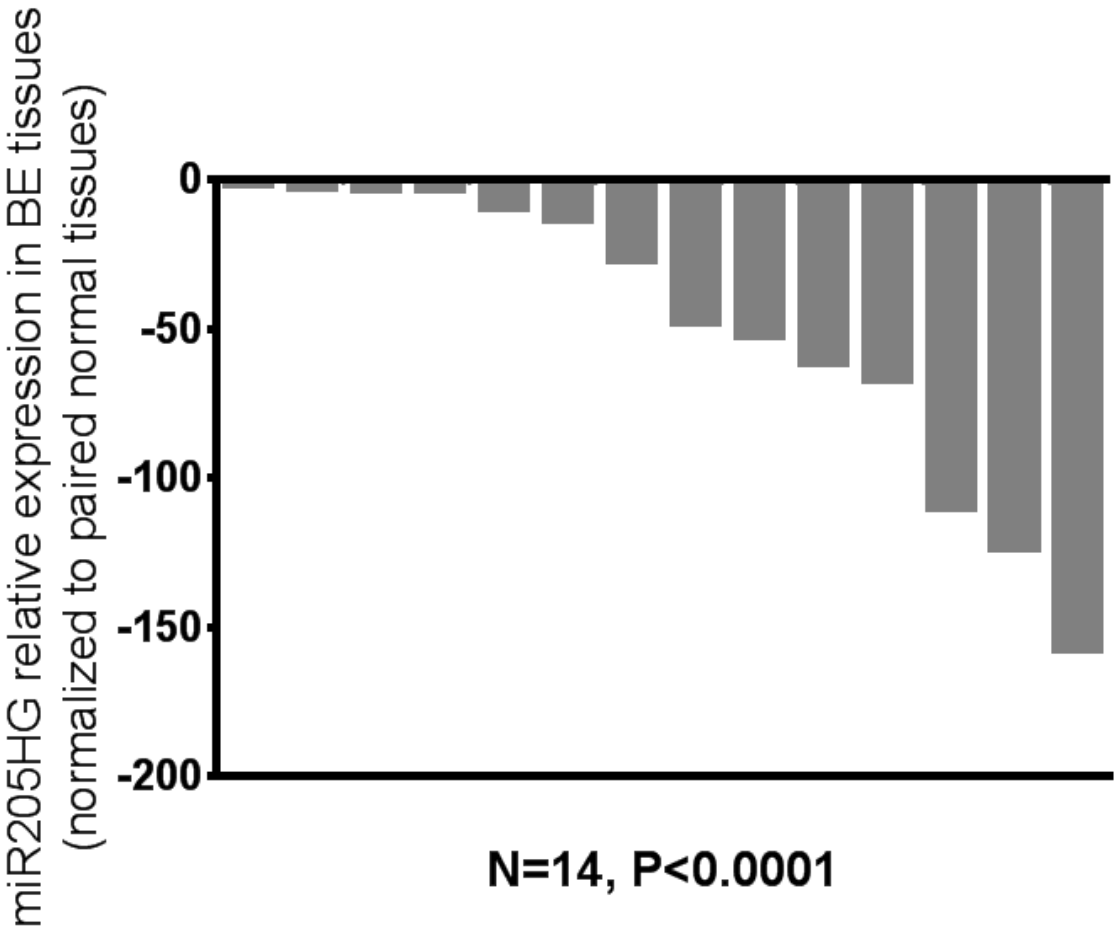

14 matched NE-BE tissue pairs were tested for miR205HG expression by qRT-PCR. It was also downregulated relative to NE in all BEs studied (14/14, average fold-change 48.3, paired t-test p-value <0.0001).

Figure 1.5

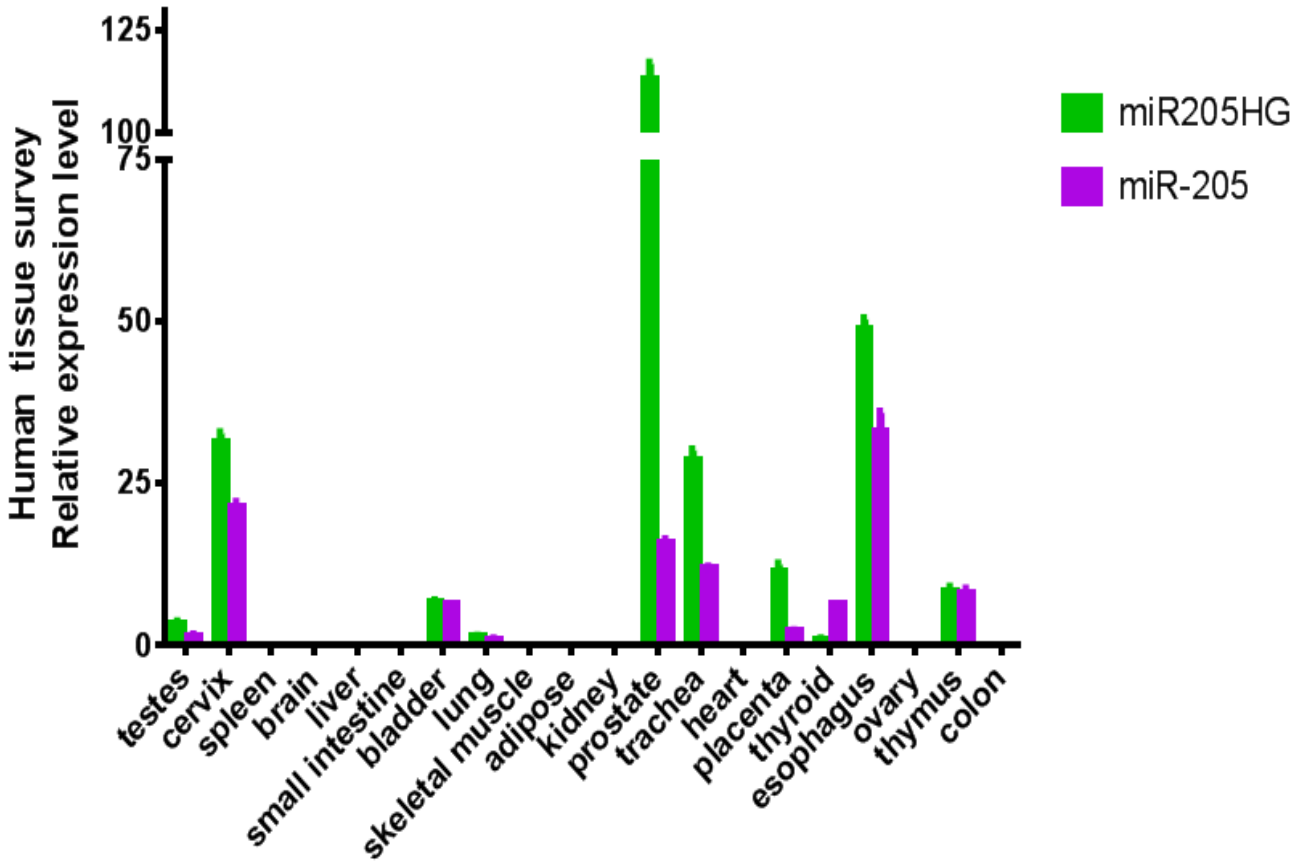

20 different normal human tissues were tested for miR205HG expression by qRT-PCR. In addition to normal esophageal tissue, miR205HG was widely expressed in normal cervix, prostate, trachea, and thymus.

Figure 2.1

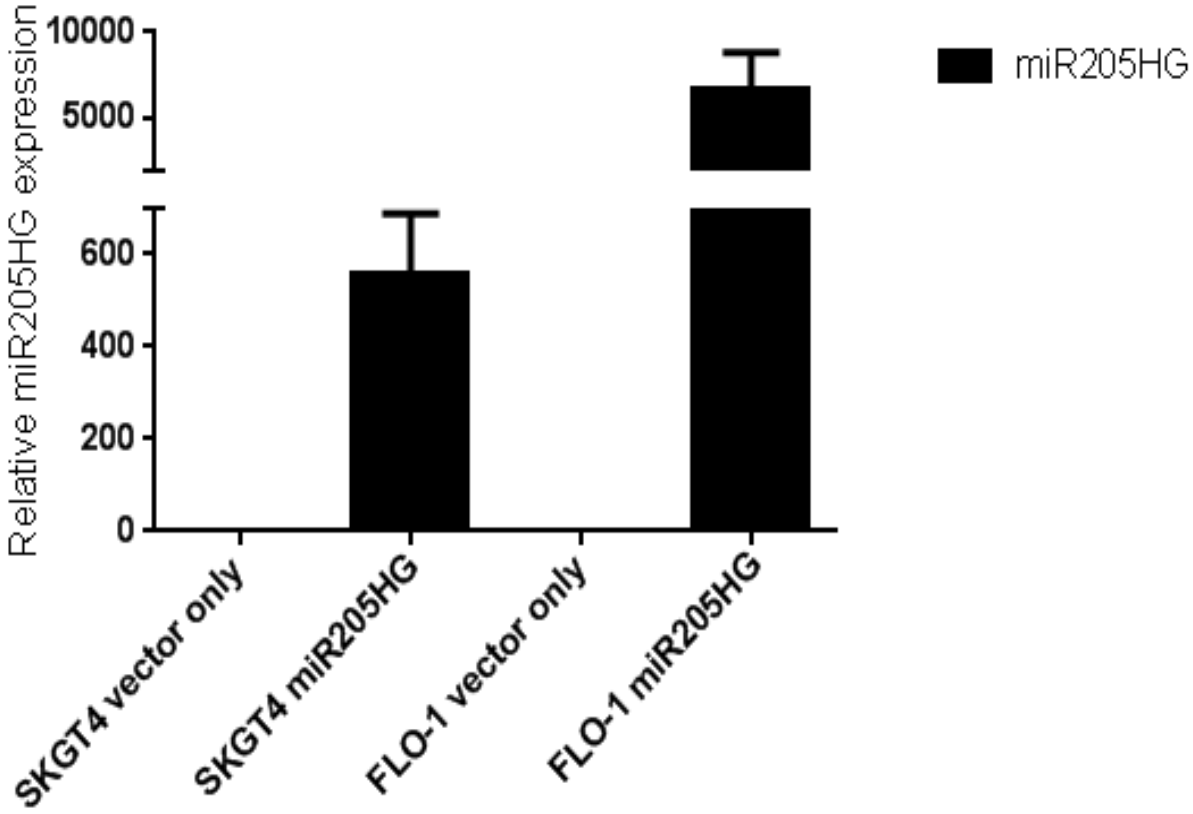

SKGT4 and FLO-1 miR205HG-stably transfected cell lines; qRT-PCR experiments confirmed miR205HG overexpression in both of these cell lines relative to vector-only transfected cells.

Figure 2.2

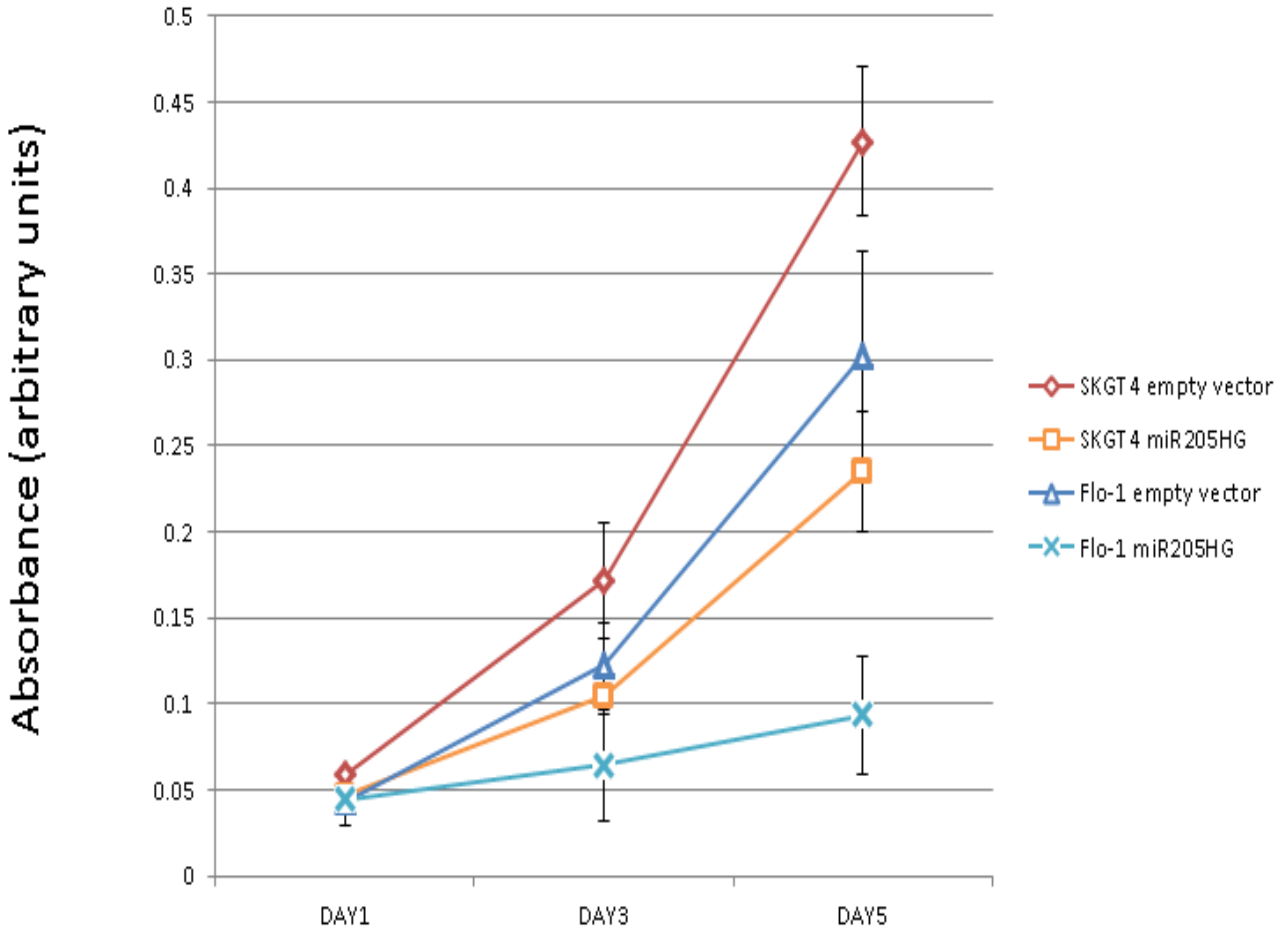

miR205HG-stable clones were used in WST-1 assays to detect the effect of miR205HG overexpression on proliferation of the EAC cell lines, SKGT4 and FLO-1. Compared to vector-only transfected negative control, forced overexpression of miR205HG decreased cell proliferation on Day 5 by 45% and 69% in SKGT4 and FLO-1 cells, respectively (p-values all <0.001).

Figure 2.3

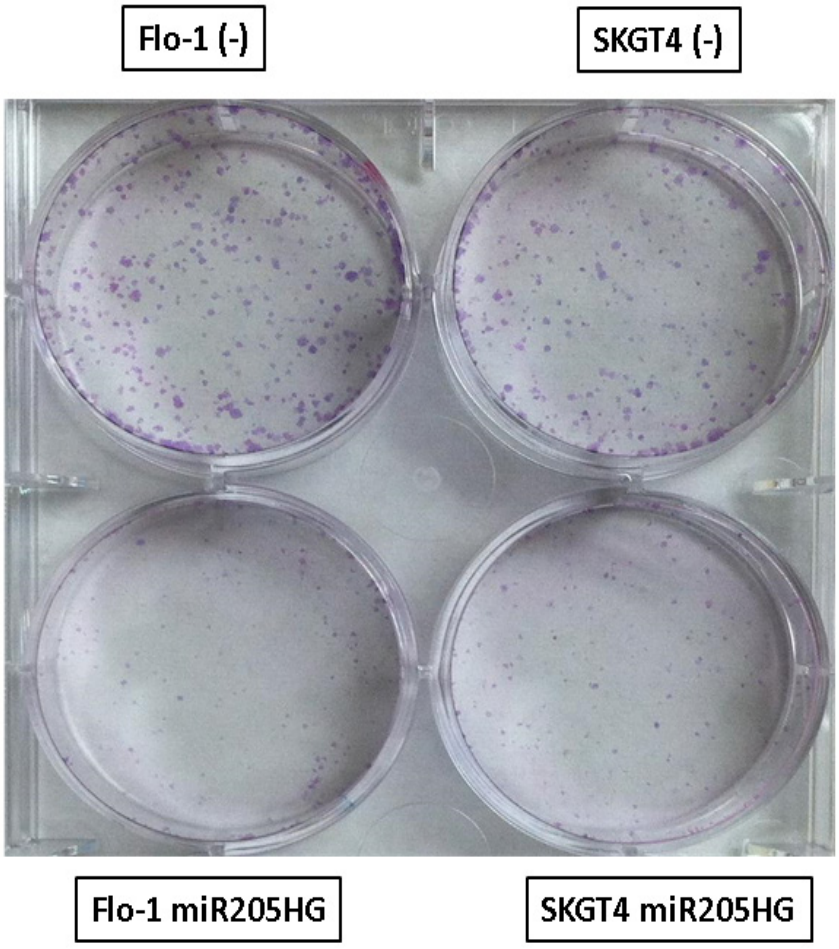

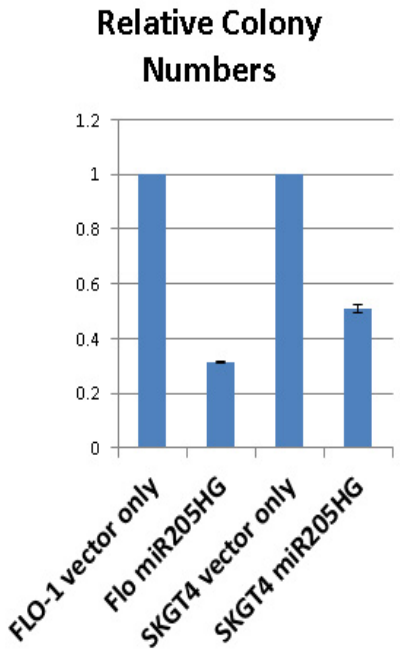

Clonogenic assays revealed that miR205HG overexpression caused a substantial reduction in colony formation in the SKGT4 (49% reduction; p-value <0.02) and FLO-1 (69% reduction; p-value <0.01) cell lines.

Figure 2.4

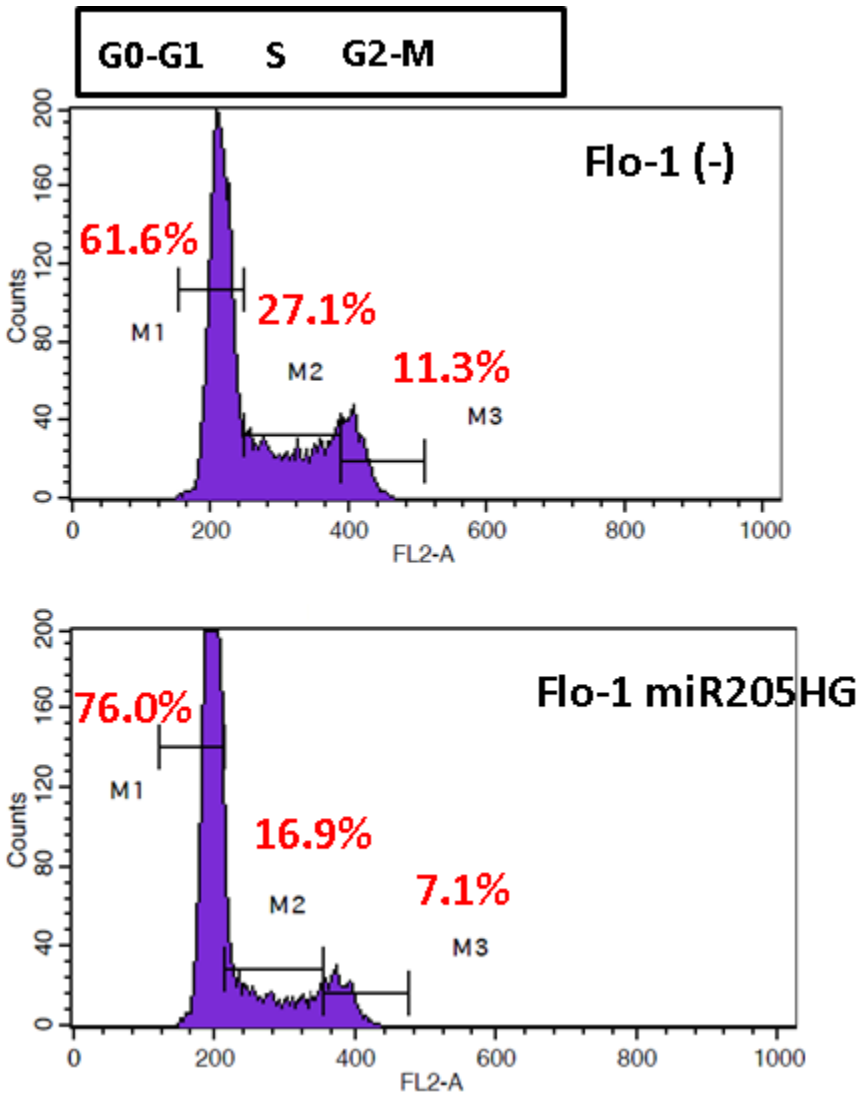

Flow cytometric cell cycle assays demonstrated that relative to empty-vector transfected control cells, miR205HG overexpression led to an accumulation of cells at G0/G1-phase and a decrease in cells at S-phase.

Figure 2.5

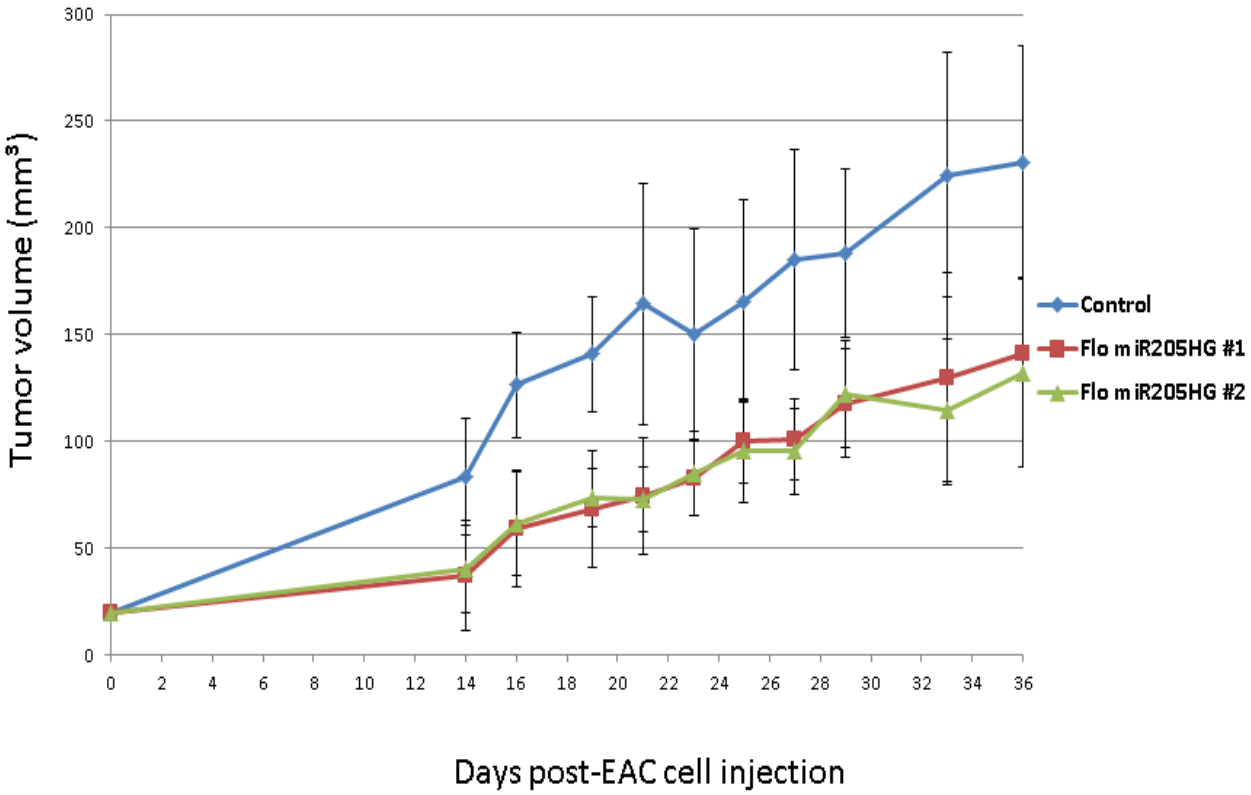

A total of 15 mice were evenly divided into 3 groups: mice were injected with either stable cells with no insert (control group) or with a miR205HG insert (2 treated groups) and were observed for 36 days. Treated animals began to show significantly smaller tumors on day 14 (control *vs.* treatment group 1, p-value =0.003; control *vs.* treatment group 2, p-value = 0.004) onward to day 36 (control *vs.* treatment group 1, p-value =0.031; control *vs.* treatment group 2, p-value = 0.017).

Figure 2.6

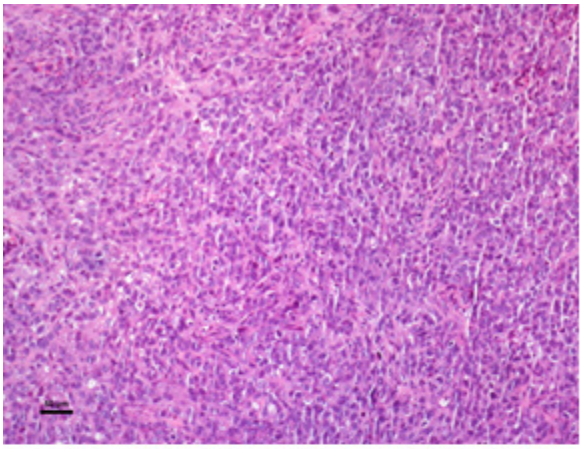

Control

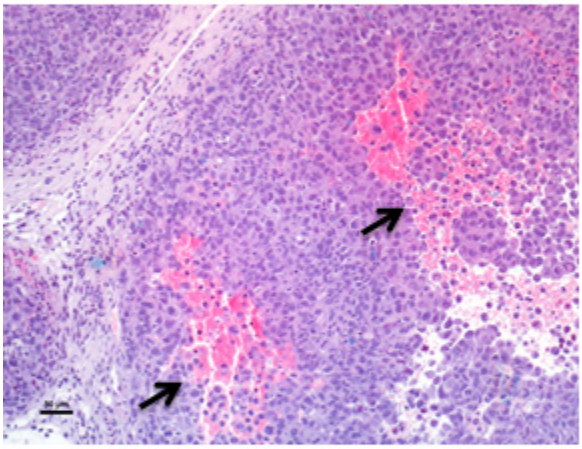

Treatment Group 1
(miR205HG #1)

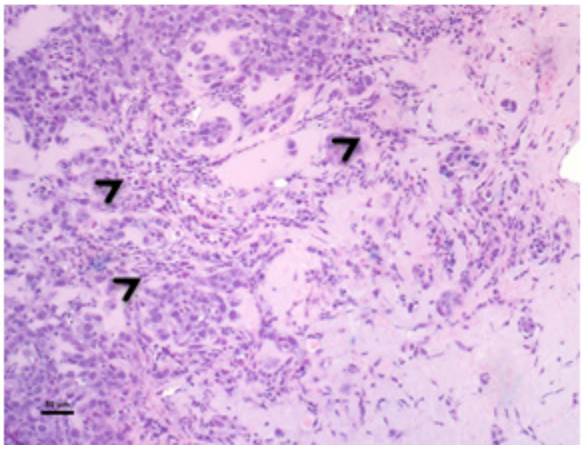

Treatment Group 2
(miR205HG #2)

Xenografts from controls were composed of densely packed sheets of cells with only occasional individual cell necrosis and leukocyte infiltration. Treated xenografts had

areas of hemorrhage and necrosis (arrows) with leukocyte infiltration (miR205HG #1) or areas of tumor cell loss, accumulation of proteinaceous fluid, leukocyte infiltration and necrotic tumor cells (arrowheads) (miR205HG #2). Scale bars = 50 um

Figure 3.1

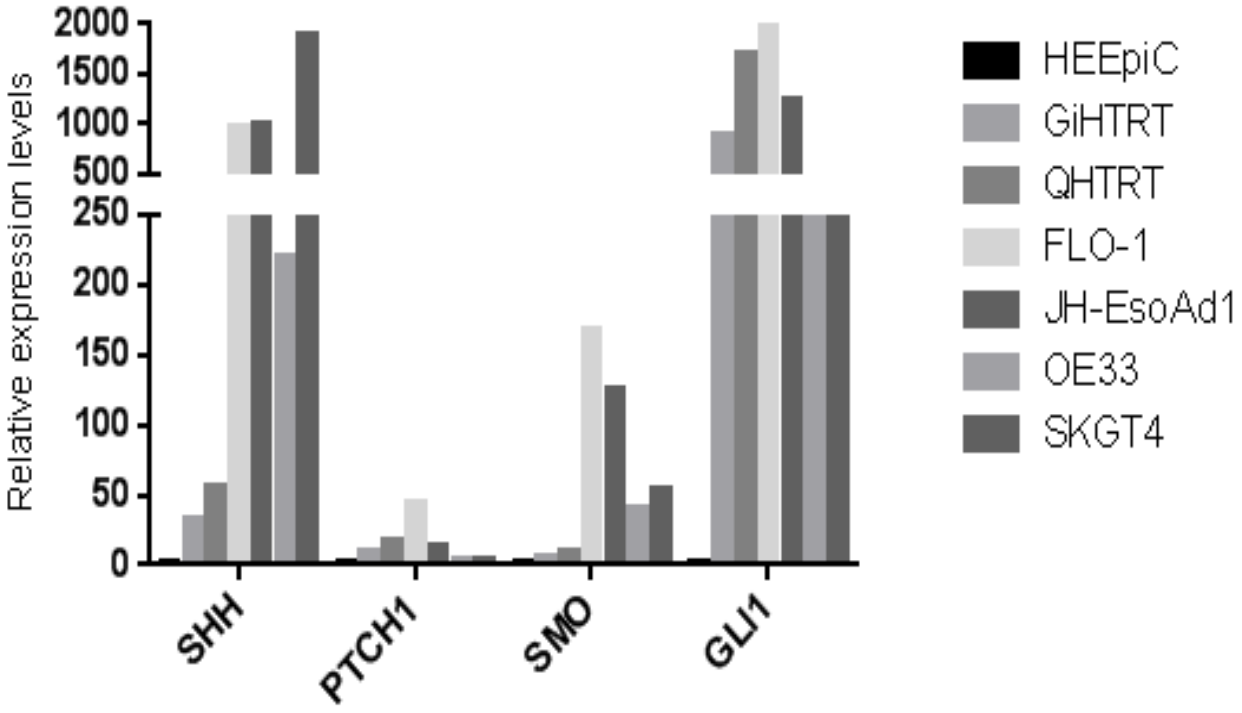

qRT-PCR of BE and EAC cell lines versus primary NE (HEEpiC) revealed that RNA expression levels of the key SHH pathway genes SHH, PTCH1, SMO, and GLI1 were upregulated in both BE (GiHTRT and QHTRT) cell lines and in all 4 EAC (FLO-1, JH-EsoAd1, OE33, and SKGT4) cell lines.

Figure 3.2

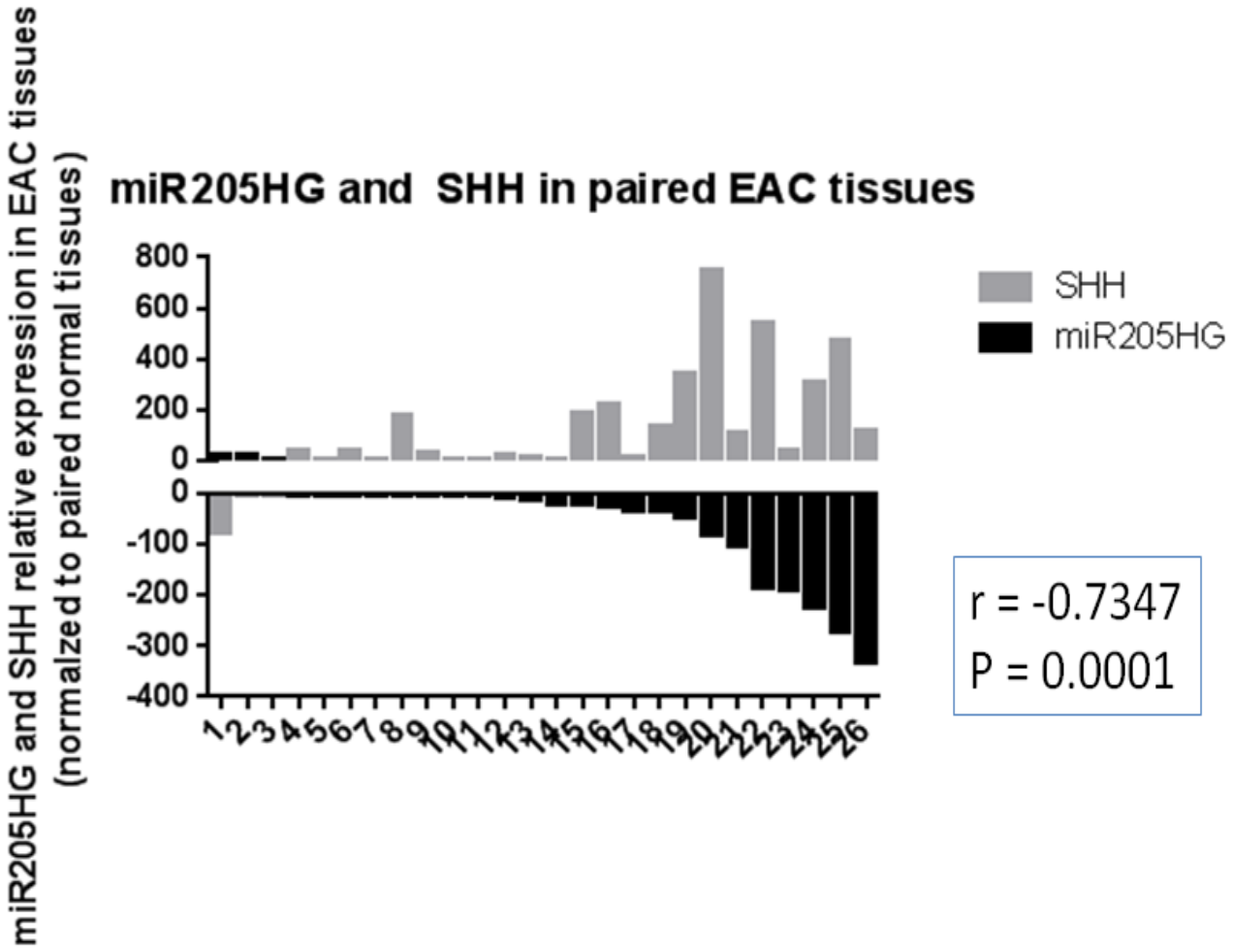

26 EAC patients that had already been tested for miR205HG expression were also tested for SHH expression by qRT-PCR. SHH expression was upregulated relative to NE in the majority of EACs studied (23/26, average fold-change 154.7, paired t-test p-value <0.0001). miR205HG and SHH expression levels were inversely correlated (r = -0.73, p-value = 0.0001).

Figure 3.3

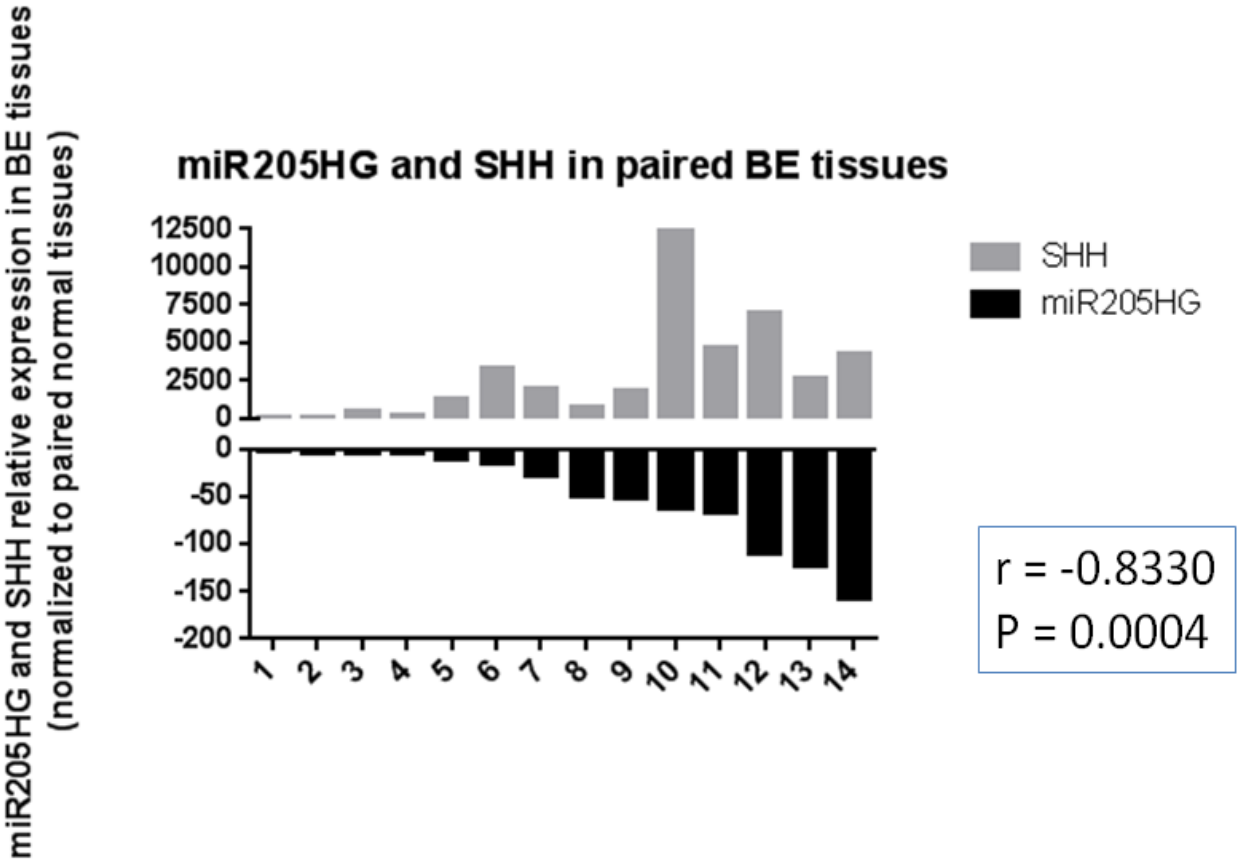

14 patients with BE were tested by qRT-PCR, and SHH was upregulated relative to NE in all BEs studied (14/14, average fold-change 2,913.0, paired t-test p-value <0.0001). miR205HG and SHH expression levels were inversely correlated (r = -0.83, p-value = 0.0004).

Figure 3.4

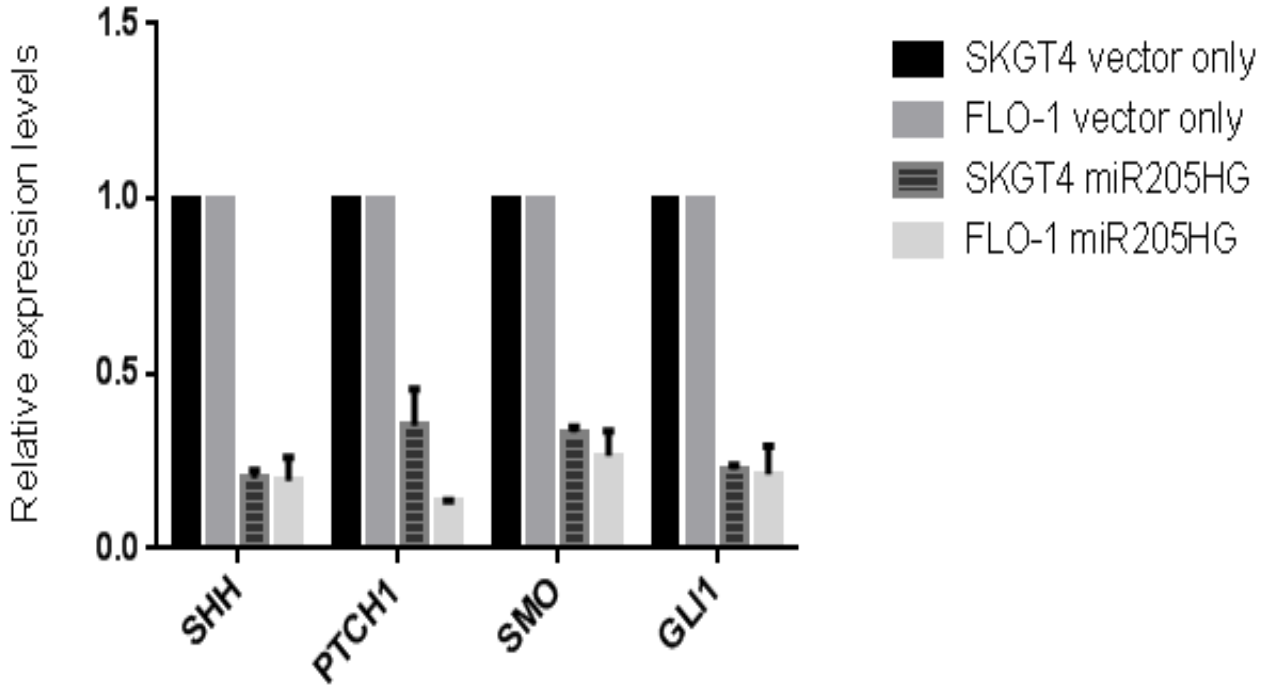

Relative to vector-only transfected negative control, qRT-PCR results from miR205HG-stable EAC clones showed significant reductions in SHH, PTCH1, SMO, and GLI1 expression levels in both SKGT4 and FLO-1 cells (p-values for all < 0.05).

Figure 3.5

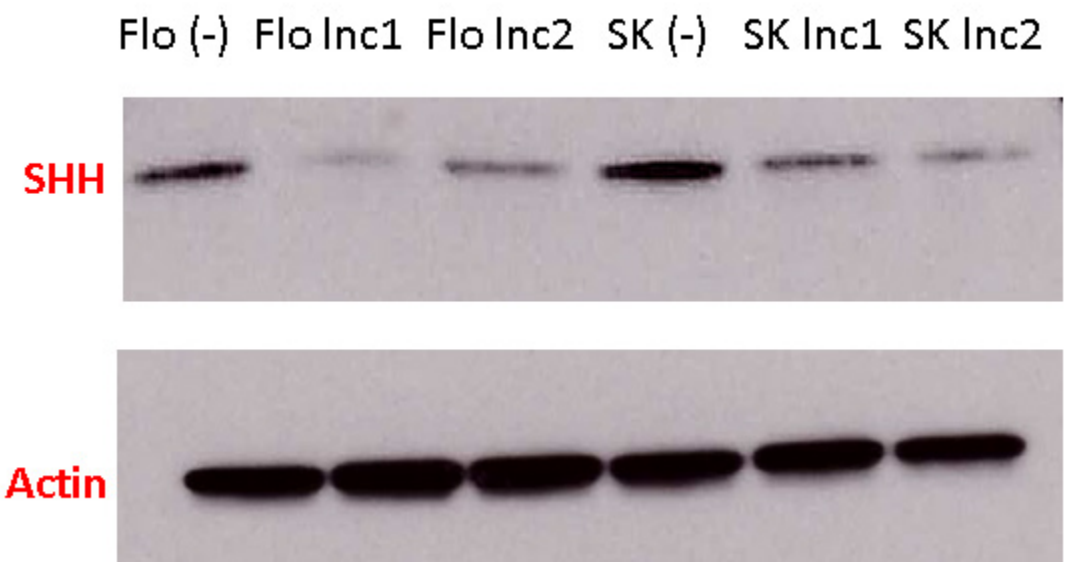

Western blot results demonstrated that SHH protein levels were greatly reduced in SKGT4 and FLO-1 miR205HG-stable clones. Flo (-) and SK (-) are FLO-1 and SKGT4 cells stably transfected with empty vectors only. Flo lnc1 and lnc2 are two different FLO-1 miR205HG stable clones (same labeling applies to SKGT4 cells).

Figure 3.6

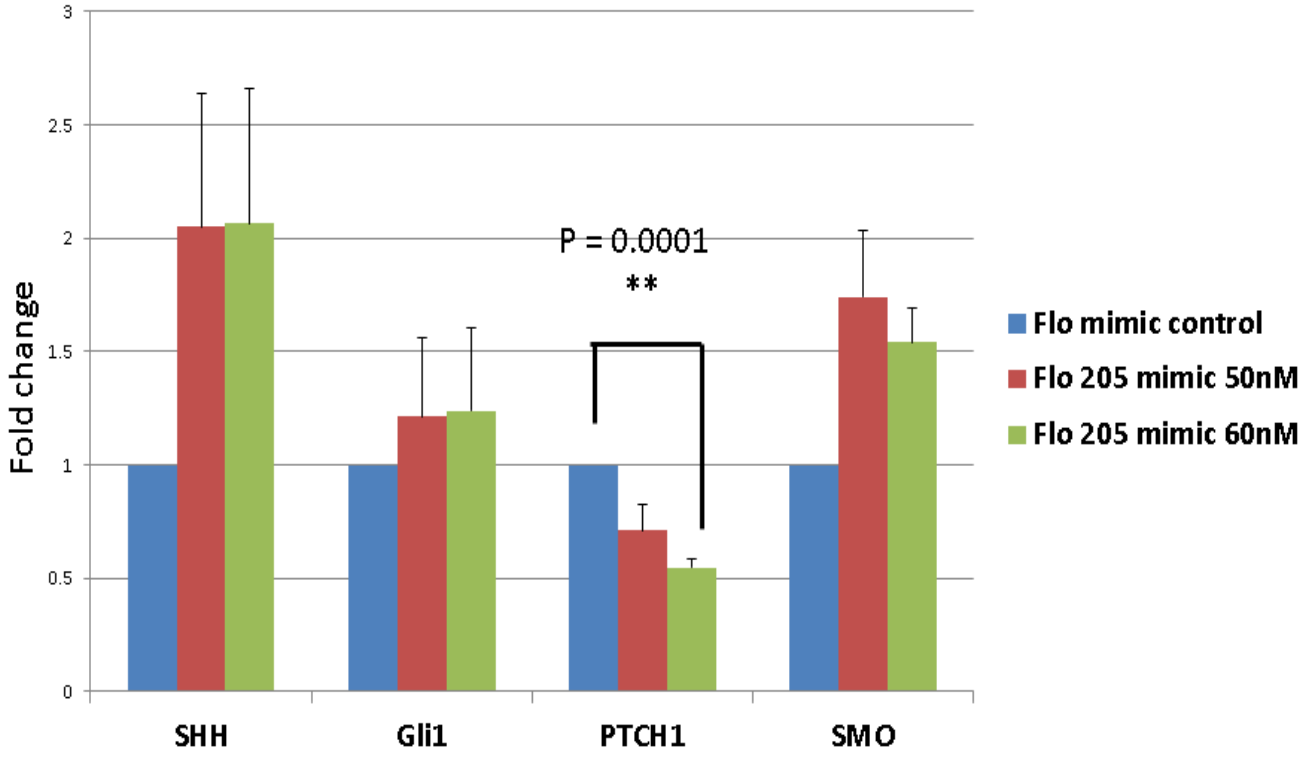

After transfecting FLO-1 EAC cells with a negative control mimic or a miR-205 mimic, qRT-PCR experiments were done to test four genes (SHH, PTCH1, SMO, GLI1). Only PTCH1 showed a significant (p-value = 0.0001) reduction when transfected with 60 nM of miR-205 mimic.

Figure 3.7

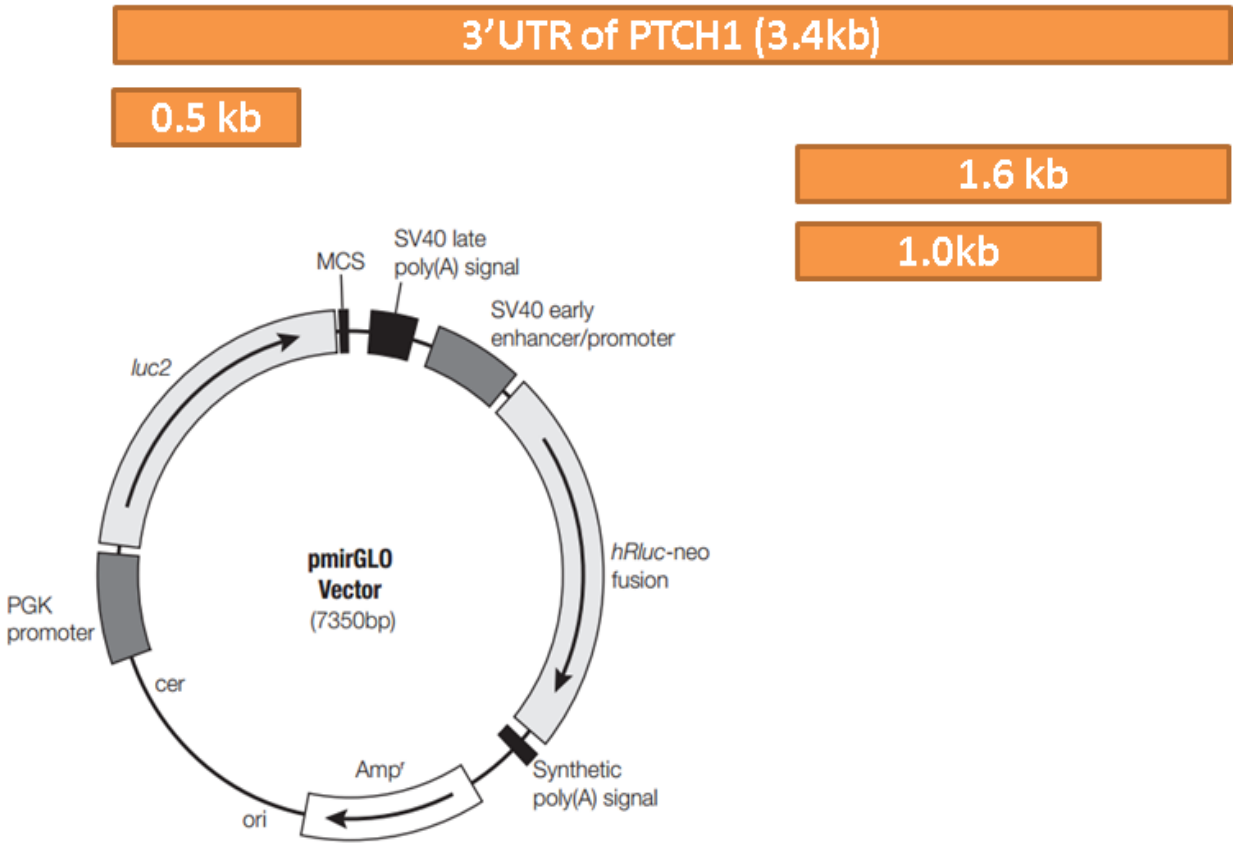

The overall PTCH1 3'UTR luciferase vector design is shown above. One full-length PTCH1 3'UTR and three different truncated versions were constructed and then cloned into vector pmirGLO.

Figure 3.8

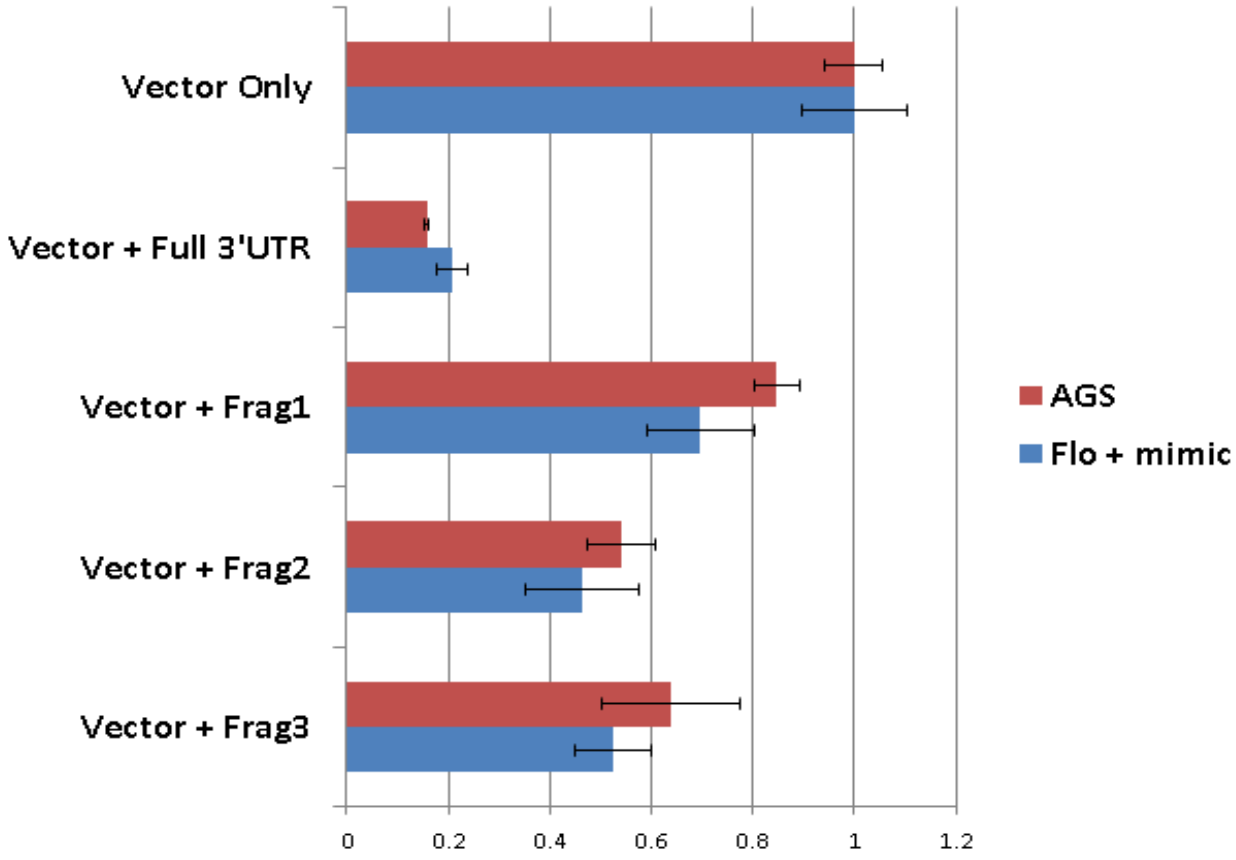

Relative to luciferase activity detected after pmiRGLO vector-only transfection, the full-length 3'UTR insert caused the most significant reduction of luciferase activity in both FLO-1 and AGS cells. Vector + Frag1, 2, and 3 denote the three different truncated PTCH1 3'UTR constructs.

CURRICULUM VITAE

Jee Hoon Song

jsong37@jhmi.edu

Education

Johns Hopkins University School of Medicine **2009 - 2015**
Ph.D.: Cellular and Molecular Medicine Program

University of California, Los Angeles (UCLA) **2002 - 2007**
B.S.: MIMG (Microbiology, Immunology, Molecular Genetics)
Minor in Classical Civilization

Research Experience

Johns Hopkins University School of Medicine, Department of Medicine, Division of Gastroenterology

2010 - 2015

- Thesis Mentor: Stephen J. Meltzer
- Dissertation Title: Novel Long Non-coding RNA Mir205HG: An Esophageal Tumor-suppressive Hedgehog Inhibitor
- Developing circulating microRNA biomarkers for Barrett's esophagus (BE) and esophageal adenocarcinoma.
- Understanding the molecular mechanistic involvement of long noncoding RNAs in BE-associated esophageal neoplasia.

Cedars-Sinai Medical Center, Department of Hematology/Oncology

2004 - 2009

- Principal Investigator: H. Phillip Koeffler
- Mutational analysis in adult T-cell and B-cell acute lymphocytic leukemias.
- Identification of epigenetically silenced genes in human pancreatic cancer cells.
- Drug antiproliferative effect on human pancreatic cancer cells.
- Single nucleotide polymorphism genomic arrays (SNP-chip) analysis in acute myeloid leukemia.

Publications

Yang X*, **Song JH***, Verma A, Wu W, Cheng Y, Bhagat T, Yu Y, Abraham JM, Ibrahim S, Yang X, Meltzer SJ: Long Noncoding RNA HNF1A-AS1 Regulates Proliferation and Migration in Esophageal Adenocarcinoma Cells. *Gut* 2014 Jun;63(6):881-90. doi: 10.1136/gutjnl-2013-305266. Epub 2013 Sep 2
* = co-first authors.

Wu W, Bhagat TD, Yang X, **Song JH**, Cheng Y, Agarwal R, Abraham JM, Ibrahim S, Hussain Z, Suzuki M, Yu Y, Eng C, Greally J, Verma A, Meltzer SJ: Hypomethylation of Noncoding DNA Regions and Overexpression of the Long Noncoding RNA, AFAP1-AS1, in Barrett's Esophagus and Esophageal Adenocarcinoma. *Gastroenterology* 2013 Jan 16.

Song JH, Meltzer SJ: MicroRNAs in pathogenesis, diagnosis, and treatment of gastroesophageal c ancers. *Gastroenterology* 2012 Jul;143(1):35-47.e2.

Agarwal R, Jin Z, Yang J, Mori Y, **Song JH**, Kumar S, Sato M, Cheng Y, Olaru AV, Abraham JM, Verma A, Meltzer SJ: Epigenomic program of Barrett's-associated neoplastic progression reveals possible involvement of insulin signaling pathways. *Endocr Relat Cancer* 2012 Feb 13;19(1):L5-9.

Orloff M, Peterson C, He X, Ganapathi S, Heald B, Yang YR, Bebek G, Romigh T, **Song JH**, Wu W, David S, Cheng Y, Meltzer SJ, Eng C: Germline mutations in MSR1, ASCC1, and CTHRC1 in patients with Barrett esophagus and esophageal adenocarcinoma. *JAMA* 2011 Jul 27;306(4):410-9.

Akagi T, Thoennissen NH, George A, Crooks G, **Song JH**, Okamoto R, Nowak D, Gombart AF, Koeffler HP: In vivo deficiency of both C/EBPβ and C/EBPε results in highly defective myeloid differentiation and lack of cytokine response. *PLoS One* 2010 Nov 3;5(11):e15419.

Akagi T, Shih LY, Ogawa S, Gerss J, Moore SR, Schreck R, Kawamata N, Liang DC, Sanada M, Nannya Y, Deneberg S, Zachariadis V, Nordgren A, **Song JH**, Dugas M, Lehmann S and Koeffler HP. Single nucleotide polymorphism genomic arrays analysis of t(8;21) acute myeloid leukemia cells. *Haematologica* 2009; 94: 1301-1306.

Thoennissen NH, Iwanski GB, Doan NB, Okamoto R, Lin P, Abbassi S, **Song JH**, Yin D, Toh M, Xie WD, Said JW, Koeffler HP: Cucurbitacin B induces apoptosis by inhibition of the JAK/STAT pathway and potentiates antiproliferative effects of gemcitabine on pancreatic cancer cells. *Cancer Res* 2009 Jul 15;69(14):5876-84.

Akagi T, Yin D, Kawamata N, Bartram CR, Hofmann WK, **Song JH**, Miller CW, Den Boer ML, Koeffler HP: Functional analysis of a novel DNA polymorphism of a tandem repeated sequence in the asparagine synthetase gene in acute lymphoblastic leukemia cells. *Leukemia Res* 2009 Jul;33(7):991-6.

Kumagai T, Akagi T, Desmond JC, Kawamata N, Gery S, Imai Y, **Song JH**, Gui D, Said J, Koeffler HP: Epigenetic regulation and molecular characterization of C/EBPalpha in pancreatic cancer cells. *Int J Cancer* 2009 Feb 15;124(4):827-33.

Song JH, Schnittke N, Zaat A, Walsh CS, Miller CW: FBXW7 mutation in adult T-cell and B-cell acute lymphocytic leukemias. *Leuk Res* 2008 Nov;32(11):1751-5.

Posters

Song JH, Cheng Y, Abraham JM, Meltzer SJ. Long non-coding RNA SS-001 regulates proliferation, cell cycle, and migration in esophageal adenocarcinoma cells. [abstract]. In: Proceedings of the 104th Annual Meeting of the American Association for Cancer Research; 2013 Apr 6-10; Washington, DC. Abstract nr 1839

Song JH, Cheng Y, Yang J, Wu W, Mori Y, Olaru AV, Bootwalla M, Sharpf R, Meltzer SJ. Circulating miRNAs as noninvasive biomarkers in esophageal adenocarcinoma patients. [abstract]. In: Proceedings of the 102nd Annual Meeting of the American Association for Cancer Research; 2011 Apr 2-6; Orlando, FL. Philadelphia (PA): AACR; Cancer Res 2011;71(8 Suppl):Abstract nr 4960

Song JH, Schnittke N, Zaat A, Walsh C, Miller CW. FBXW7 Mutation occurs in adult T-cell and acute lymphocytic leukemias. [abstract]. In: Proceedings of the 97th Annual Meeting of the American Association for Cancer Research; 2006 Apr 1-5; Washington, DC. Philadelphia (PA): AACR; 2006; No. 1, p. 780: Abstract nr 3322

U.S. Patent Applications

Pub. No.: WO/2012/012689
International Application No.: PCT/US2011/044963
Circulating MicroRNAs are Biomarkers of Various Diseases.
Inventors: **Song JH**, Cheng Y, Meltzer SJ. Filed: Jul. 22, 2011.

Pub. No.: WO/2012/135091
International Application No.: PCT/US2012/030518
Serum-based miRNA Microarray and its Use in Diagnosis and Treatment of Barrett's Esophagus (BE) and Esophageal Adenocarcinoma (EAC).
Inventors: **Song JH**, Cheng Y, Meltzer SJ. Filed: Mar. 26, 2012.